# Chapter 4 TEMPO Decay in Acid at High Temperature

## 4.1. Introduction

In chapter 3, TEMPO decay in acid was investigated. At room temperature, the reaction involves disproportionation which is well understood. The kinetic profile of TEMPO decay at room temperature fits the kinetic model of disproportionation accurately. However, TEMPO decay at high temperature was complicated. In order to simplify the system and avoid potential reactions with organic substrate, TEMPO decay was studied in aqueous $H_2SO_4$. TEMPO decay at high temperature is thus likely to involve side reactions of TEMPO or further reactions of the disproportionation products.

Thermal stability of TEMPO was studied[1] in various solvents. TEMPO is stable in solvents lacking H-donating capacity at 150 ℃. However, in H-donor solvents, TEMPO can be reduced to form the corresponding hydroxylamine (TEMPOH) and amine (TEMPH) under thermal conditions (Scheme 4.1).
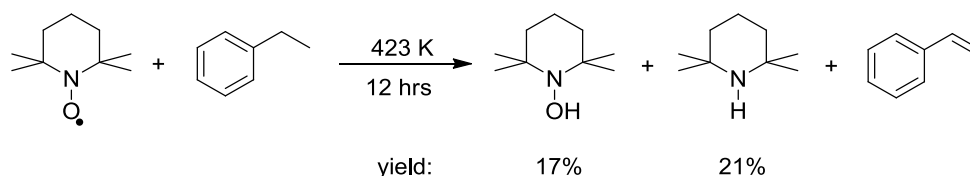


**Scheme 4. 1. Thermal decomposition of TEMPO in ethylbenzene at 150 ℃.**

At higher temperature (e.g. 230 ℃), hydrogen abstraction between TEMPO molecules followed by elimination reaction leads to formation of methyl radical and the corresponding nitroxide. The highly-reactive methyl radical then undergoes various subsequent reactions leading to formation of alkoxyamine, peroxyl radical and another nitroxide radical (Scheme 4.2).
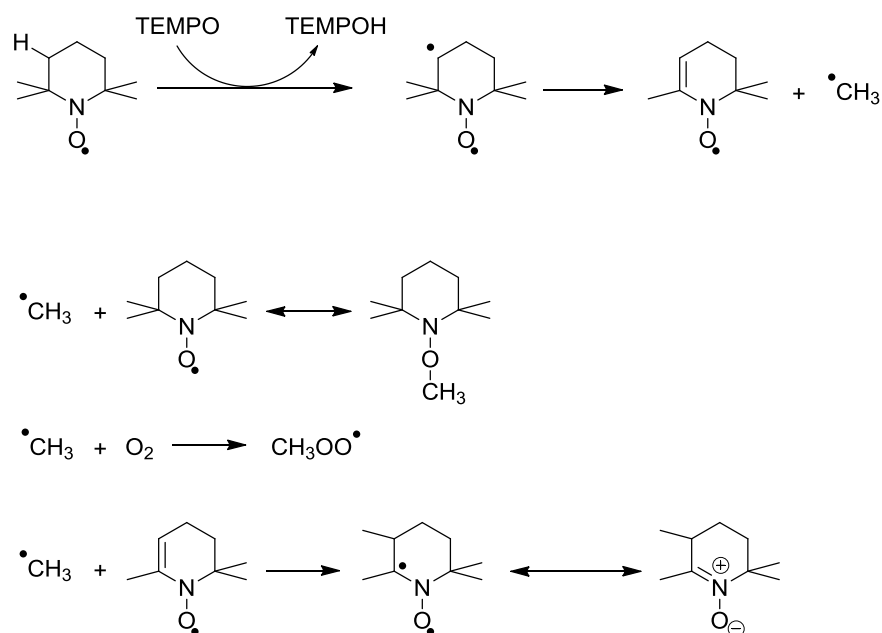
**Scheme 4. 2. Hydrogen abstraction between TEMPO molecules at above 230 ℃ and subsequent reactions of methyl radical.**

The decomposition of TEMPO could be the side reactions which we observed along with acid-catalyzed TEMPO disproportionation at high temperature. However, the temperature is much lower (e.g. lower by 130-150 ℃) in our case.

Decomposition of N-oxoammonium salt could also explain TEMPO decay at high temperature. Golubev *et al.* suggested[2] that N-oxoammonium cation could hydrolyze and form TEMPO and hydroxyl radical (Scheme 4.3). Decomposition of oxoammonium salt could also drive TEMPO disproportionation reaction forward.
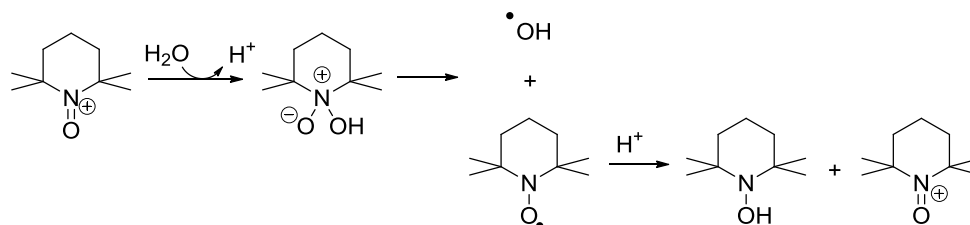


**Scheme 4. 3. Hydrolysis of N-oxoammonium cation and subsequent formation of hydroxyl radical and TEMPO.**

These reactions can in principle explain the complicated kinetic profile of TEMPO decay in acid at high temperature. However, the precise mechanism is not known.

## 4.2.   Aims and objectives

The aim of the investigation described in this chapter is to establish a detailed mechanism of TEMPO decay in acid at high temperature (e.g. 100 °C). In order to achieve this aim, possible reaction routes were considered. The complicated kinetic profiles could be explained by literature reported reactions including thermal decomposition of TEMPO and hydrolysis of oxoammonium salt. To determine the reaction mechanism, product analysis was carried out using a range of common analytical techniques.

## 4.3.   Thermal decomposition of TEMPO in acid: decomposition of N-oxoammonium salt

As discussed in Chapter 3, TEMPO decay in $H_2SO_4$ at high temperature gives complicated kinetic profiles. Significant deviation from kinetic model for disproportionation was observed (Figure 3.28, p134). In order to determine the origin of this deviation, a neutralization experiment was carried out.

### 4.3.1.   Irreversible TEMPO decay in acid at high temperature

As discussed in Section 3.4.4 (p134), TEMPO disproportionation is reversible (Scheme 4.4).
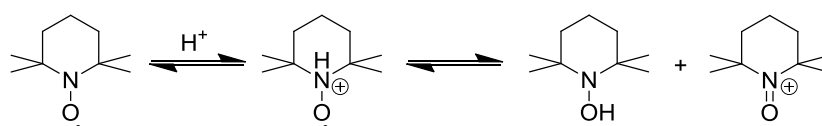


**Scheme 4. 4. Reversible TEMPO disproportionation reaction.**

Neutralization of the reaction mixture of TEMPO disproportionation at room temperature leads to nearly quantitative recovery of TEMPO regardless of reaction time (Figure 3.30, p136). This effect is due to the fast comproportionation reaction of hydroxylamine and oxoammonium salt (Scheme 4.5).
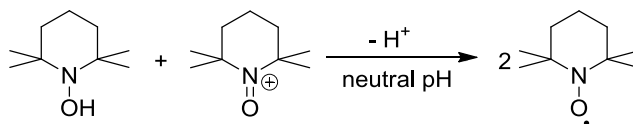


**Scheme 4. 5. Fast comproportionation reaction of hydroxylamine and oxoammonium salt at neutral pH.**

However, for TEMPO decay at high temperature, a completely different reactivity was observed. A solution of $6.4 \times 10^{-3}$ M TEMPO in 1 M $H_2SO_4$ was heated to 80 °C in a sample vial. At different reaction times, aliquots of the reaction mixture were neutralized with excess solid $NaHCO_3$. The neutralized solution was analyzed quantitatively by EPR spectroscopy to compare TEMPO concentrations. Instead of a full recovery, TEMPO intensity of neutralized reaction mixture showed a significant decay (Figure 4.1). This suggests that TEMPO decay at high temperature is not reversible.
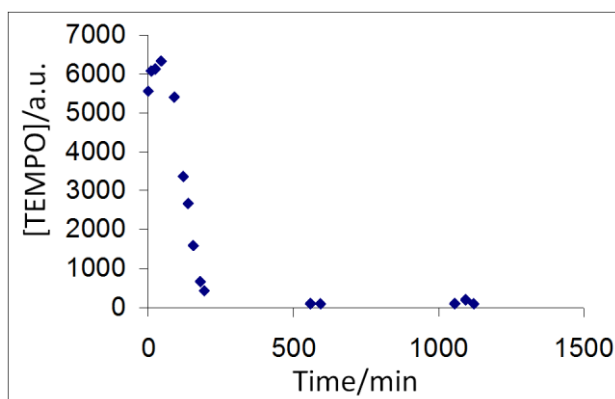


**Figure 4. 1. $6.4 \times 10^{-3}$ M TEMPO in 1M $H_2SO_4$ at 80 °C. Aliquots of reaction mixture were neutralized with excess $NaHCO_3$ at different time intervals.**

The irreversible TEMPO decay at high temperature could be due to decomposition of TEMPO or disproportionation products (e.g. oxoammonium salt). As shown in Scheme 4.1 (p144), thermal decomposition of TEMPO in ethyl benzene at 150 °C results in less than 40% decay of TEMPO after 12 hours. The decay shown in Figure

4.1 is much more significant. Therefore, the origin of this effect is unlikely to be thermal decomposition of TEMPO, but further reaction of the disproportionation product, N-oxoammonium salt.

### 4.3.2.   Thermal decomposition of N-oxoammonium salt

In order to monitor the decay of TEMPO and oxoammonium salt at high temperature, UV-*vis* spectroscopy was employed. As shown in Figure 4.2a, TEMPO and oxoammonium salt have distinctive UV absorbance at 425nm and 476nm[3], respectively. A solution of $10^{-3}$ M TEMPO in 1 M $H_2SO_4$ was heated in a sealed sample vial to 80 ℃. UV spectra of the reaction mixture were recorded at different reaction times (Figure 4.2).
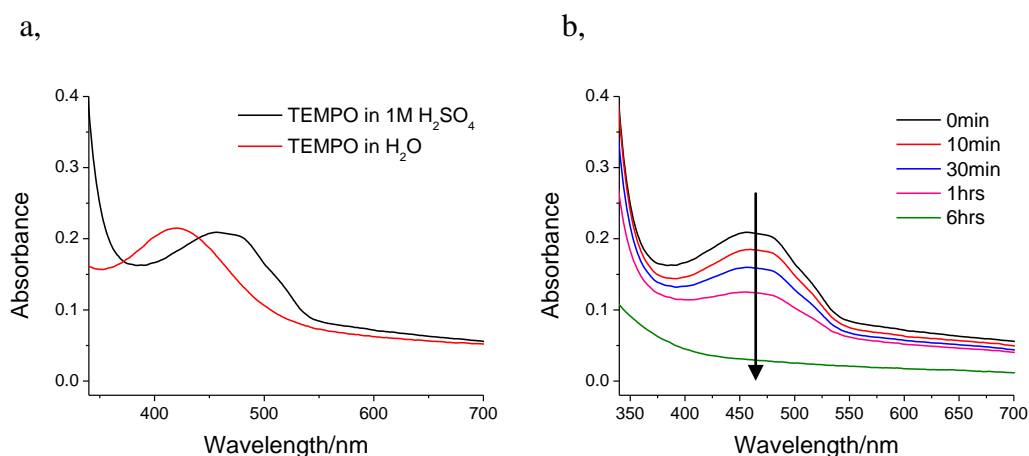


**Figure 4. 2. $10^{-3}$ M TEMPO in 1 M $H_2SO_4$ at 80 ℃ monitored by UV spectroscopy. a, UV spectrum of TEMPO in $H_2SO_4$ prior to heating in comparison with UV spectrum of TEMPO in water. This suggests the disproportionation is finished and the product present in the reaction mixture is mainly oxoammonium salt. b, Absorbance decay at 476 nm of the reaction mixture over 6 hours.**

It is evident that oxoammonium salt formed initially from TEMPO decomposes during the reaction. Its distinctive UV band at *ca.* 476 nm vanished after heating the reaction mixture for 6 hours. To confirm this observation and determine the reaction conditions, a similar experiment was carried out starting from an authentic sample of N-oxoammonium chloride. A solution of 0.52 M N-oxoammonium chloride in 1M $H_2SO_4$ was heated in a closed sample vial at 80 ℃. UV spectra of the reaction mixture were recorded at different reaction times. Decay of the distinctive UV band

at 476nm was observed, which confirms thermal decomposition of oxoammonium salt (Figure 4.3). The reaction follows a 1$^{st}$ order kinetic model. Detailed kinetic investigation on the reaction rate is discussed in Section 4.3.2.4. (p152).
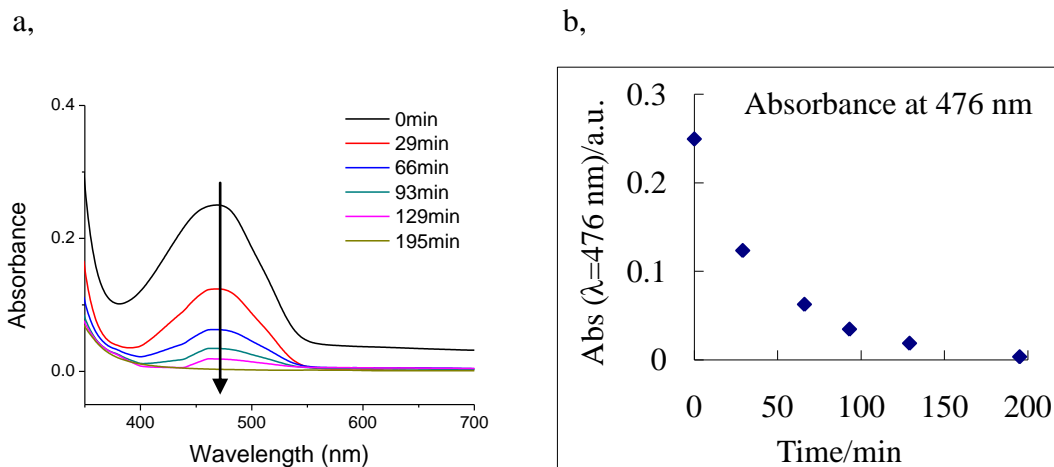
a,

b,



**Figure 4. 3. a, UV spectra of 0.52M N-oxoammonium chloride in 1M H$_2$SO$_4$ in D$_2$O at 80 ℃ at different reaction times. b, Plot absorbance vs. time.**

## 4.3.2.1. The effect of acidity on thermal decomposition of oxoammonium salt

Decomposition of oxoammonium salt is thus likely a side reaction in the decay of TEMPO in acid at high temperature. In order to explore the effect of acidity on the mechanism of thermal decomposition of oxoammonium salt, the reaction was carried out at different concentrations of acid. Solutions of 0.037 M oxoammonium chloride in different concentrations of H$_2$SO$_4$ were heated to 100 ℃ and monitored by UV-*vis* spectroscopy over time (Figure 4.4). The absorbance decay was normalized by manually subtracting the baseline to give a better kinetic profile.
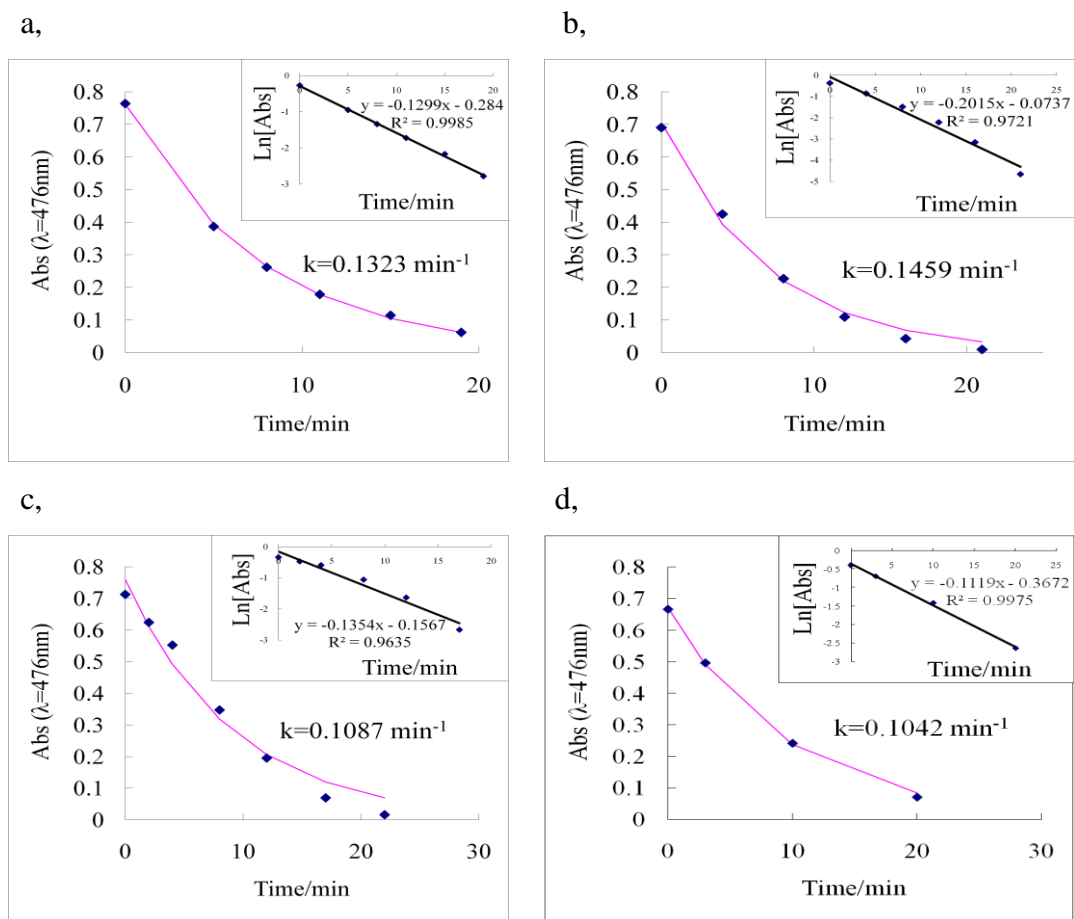
a,



b,



c,



d,



**Figure 4. 4. Absorbance decay at 476 nm of 0.037 M oxoammonium chloride in different concentrations of H₂SO₄ at 100 ℃. a, in 1 M H₂SO₄. b, in 0.5 M H₂SO₄. c, in 0.1 M H₂SO₄. d, in H₂O.**

As shown in Figure 4.4, kinetic profiles of TEMPO oxoammonium salt decomposition with different acidity give reasonable fit to 1st-order kinetic model. The rate constants obtained from fitting are believed to be the same within experimental error. The fairly large error is probably due to solvent effect. The acidities of the solvents are very different which may lead to different reaction rate. Another source of error is the data treatment. The baseline of UV spectra was subtracted manually which may have caused inconsistency. However, even if the rate constant obtained from this experiment may not be very accurate, the data convincingly show that this reaction follows 1st-order kinetics and the reaction is not acid-catalyzed.

**4.3.2.2.** **The effect of $O_2$ on thermal decomposition of oxoammonium salt**

Observation of oxoammonium salt decomposition raises a question as to whether this reaction interferes with the oxygen consumption measurements. If oxygen is involved in the oxoammonium salt decomposition process, then $O_2$ consumption of nitroxide in acidic monomers is no longer comparable to that in neutral monomers. To answer this question, N-oxoammonium salt decomposition was studied in the absence of $O_2$. A solution of 0.037 M oxoammonium chloride in $H_2O$ was deoxygenated by nitrogen gas. This solution was heated to 100 °C. Since it is difficult to take samples for UV measurements without introducing air, only the starting point and the end point were monitored by UV instead of a full kinetic profile. However, in comparison with the same reaction in the presence of $O_2$, similar extent of decay was observed (Figure 4.5).
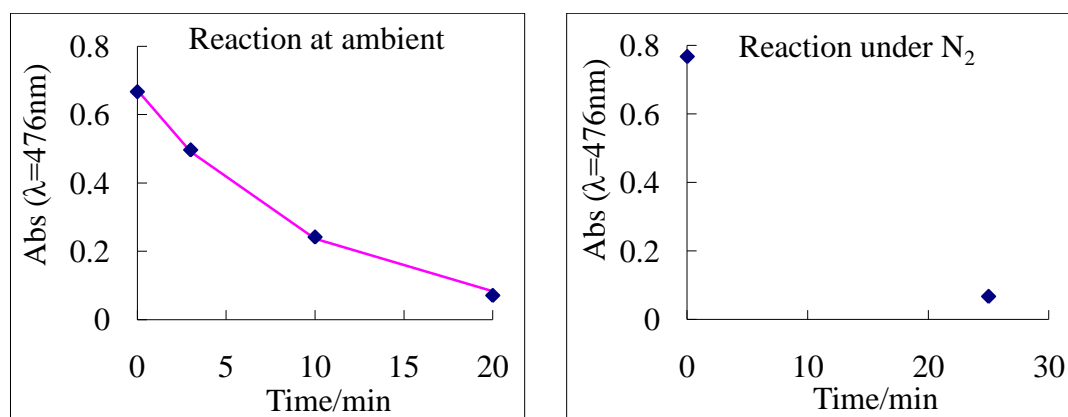


**Figure 4. 5. Absorbance decay at 476 nm of 0.037 M oxoammonium chloride in $H_2O$ at 100 °C. a, reaction carried out at ambient atmosphere. b, reaction carried out under $N_2$.**

Therefore, thermal decomposition of oxoammonium salt does not depend on the presence of oxygen.

**4.3.2.3.** **Light dependence of thermal decomposition of oxoammonium salt**

Photolysis of nitroxide radicals was reported[4] to lead to elimination of nitric oxide ($^\bullet$NO). In order to test if decomposition of oxoammonium salt is light induced, the reaction was carried out in the dark. A solution of 0.037 M oxoammonium chloride

in $H_2O$ was heated at 100 ℃ in a round-bottom flask which was covered with tin-foil. Aliquots of the reaction mixture were taken at different times and their UV-*vis* spectra were recorded. The obtained absorbance decay at 476 nm is shown in Figure 4.6. As compared with the reaction carried out under visible light, oxoammonium salt decomposition showed a similar rate. Hence, the reaction is not light-induced.
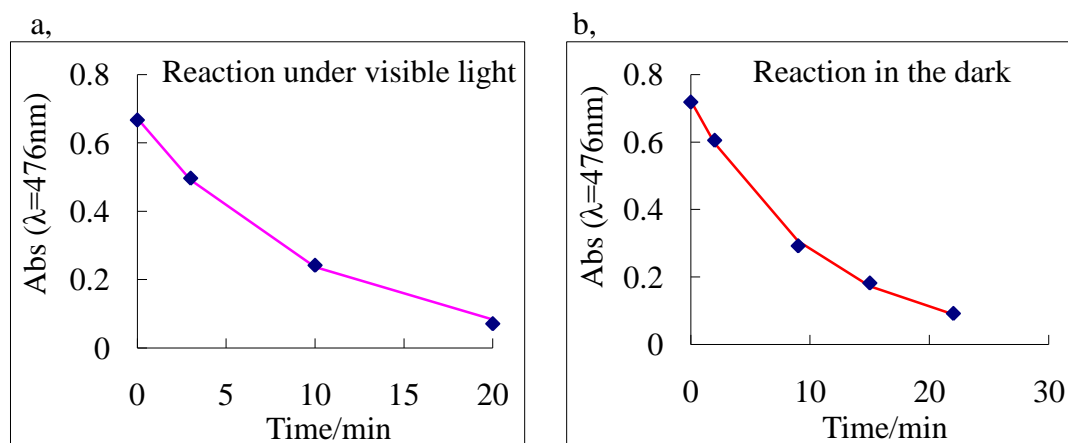
a,

b,

**Figure 4. 6. Absorbance decay at 476 nm of 0.037 M oxoammonium chloride in $H_2O$ at 100 ℃. a, reaction carried out under visible light. b, reaction carried out in the dark.**

### 4.3.2.4.       Kinetic model for thermal decomposition of oxoammonium salt

Thermal decomposition of different concentrations of N-oxoammonium chloride in $H_2O$ was studied in order to determine the kinetic order of the reaction. Solutions of 0.038 M, 0.057 M and 0.076 M oxoammonium salt in $H_2O$, were heated in sample vials to 100 ℃ and UV spectra were recorded at different reactions times. Thus, kinetic profiles of the reaction were obtained (Figure 4.7).
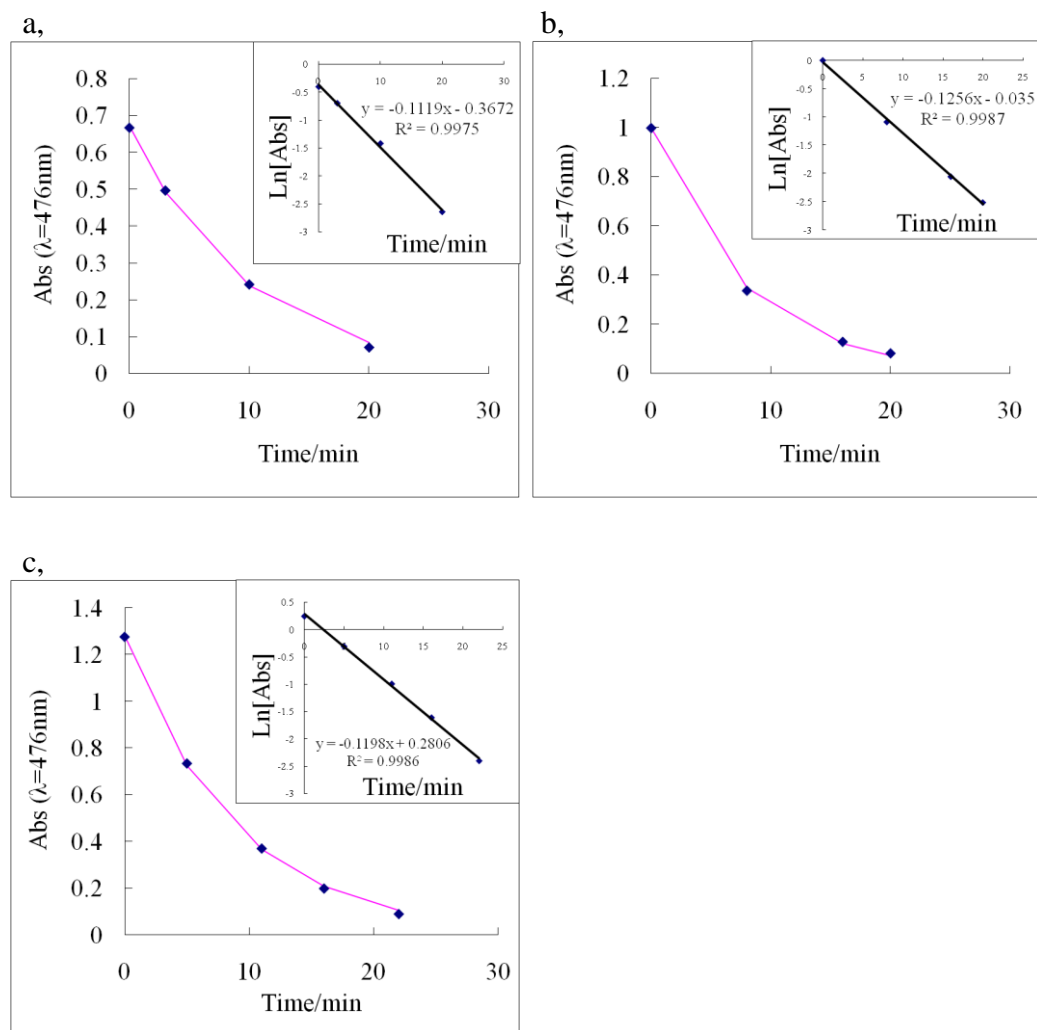
a,

b,

c,

**Figure 4. 7. Absorbance decay at 476 nm of different concentrations of oxoammonium chloride in H$_2$O at 100 ℃. a, C$_0$=0.038 M, k=0.112min$^{-1}$. b, C$_0$=0.057 M, k=0.126min$^{-1}$. c, C$_0$=0.076 M, k=0.120min$^{-1}$.**

As shown in Figure 4.7, the reaction rate does not depend on oxoammonium salt concentration. The rate was determined by fitting to 1$^{st}$-order kinetic model. The reaction rate of TEMPO oxoammonium salt decomposition at 100 ℃ is thus determined to be 0.120±0.008 min$^{-1}$.

### 4.3.3. Thermal decomposition of TEMPO in H$_2$O

Thermal decomposition of oxoammonium salt is likely to be a side reaction in the decay of TEMPO in acid at high temperature. As discussed in Section 4.1 (p144), TEMPO can also decompose at neutral pH. Therefore, thermal decomposition of

TEMPO in its aqueous solution was investigated to determine the reaction rate and its impact on the overall TEMPO decay. A solution of 0.04M TEMPO in $H_2O$ was heated in a sample vial to 100 ℃ and monitored by UV-*vis* spectroscopy. The kinetic profile is shown in Figure 4.8. The reaction rate was determined to be 0.019 $min^{-1}$ compared to 0.12 $min^{-1}$ of oxoammonium salt thermal decomposition. Oxoammonium salt decomposition is more than six times faster. Furthermore, TEMPO has a $pK_a$ of 5.5. As a result, TEMPO is partially protonated at neutral pH. Therefore, TEMPO disproportionation contributes to the decay at neutral pH.
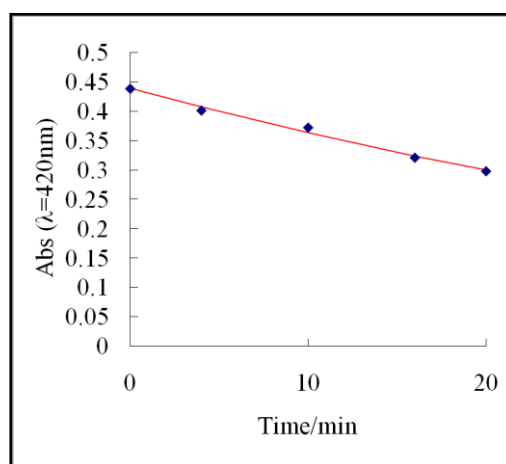


**Figure 4. 8. Absorbance decay at 420 nm of 0.04 M TEMPO in $H_2O$ at 100 ℃. The reaction rate k=0.019 $min^{-1}$.**

Hence, in order to test the persistency in neutral media, a solution of 0.038 M TEMPO in pH=7 buffer was heated to 100 ℃. The decay of TEMPO was monitored with EPR spectroscopy. The kinetic profile was obtained from double integration of exchange broadened EPR spectra of TEMPO (Figure 4.9). The result shows that TEMPO is persistent at this temperature.
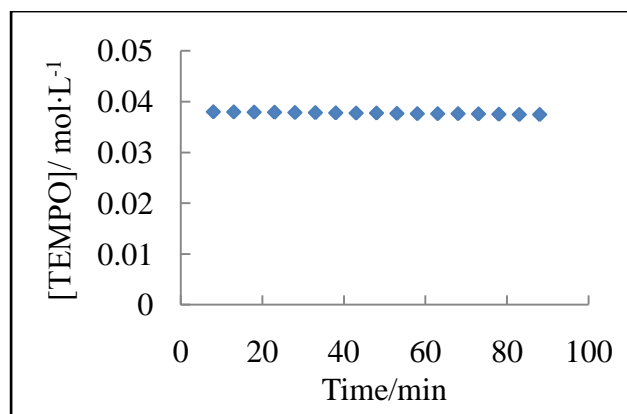
**Figure 4. 9. Persistency of TEMPO at 100 ℃ in a pH=7 buffer solution.**

Since the decay of TEMPO at 100 ℃ is slow in its aqueous solution and negligible in pH7 buffer, we thus conclude that the unusual decay of TEMPO in acid at high temperature is due to disproportionation of TEMPO and further decomposition of oxoammonium salt.

### 4.3.4. Formation of a UV-active compound in thermal decomposition of oxoammonium salt

Interestingly, in the study of oxoammonium salt decomposition in water, a new UV band at *ca.* 670 nm was observed (Figure 4.10). This band was only observed in the reactions carried out in water, but not in acid.
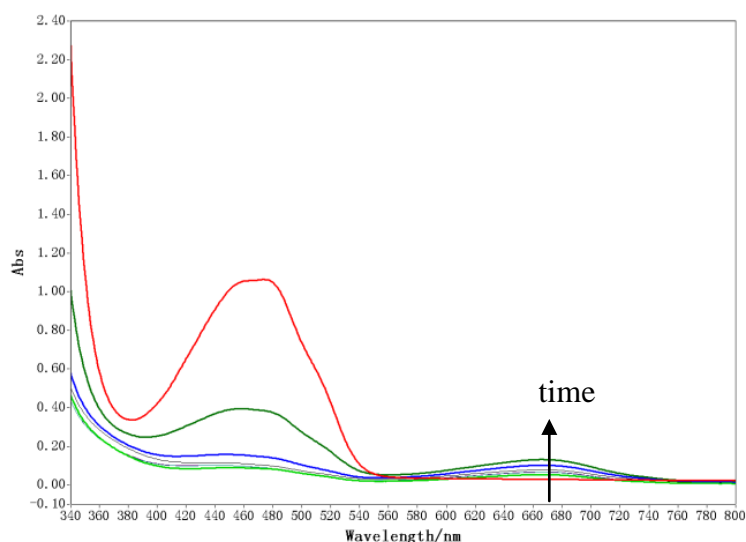


**Figure 4. 10. Increase of absorbance at 670 nm of 0.057 M oxoammonium salt in H$_2$O at 100 ℃ in 20 minutes.**

The reaction mixture, which has the UV absorbance at 670nm, was tested for its stability in acid. Introduction of dilute sulphuric acid did not result in removal of the UV band, which indicates that this product is not related to a protonation-deprotonation process. However, upon heating this reaction mixture, the UV absorbance diminished. It suggests that this UV active product is not stable in acid, which explains the absence of this band in oxoammonium salt decomposition in acidic media. This observation provides implications on the mechanism of the decomposition reaction. The absorbance at this wavelength is consistent with literature reported[5] absorbance of C-nitroso monomers, which has been assigned to an $n_N \rightarrow \pi^*$ transition.

Thermal decomposition of oxoammonium salt was thus determined to be a major side reaction of TEMPO decay in acid at high temperature. However, the fate of oxoammonium salt remains unclear. Hence, next section describes the product analysis for decomposition of oxoammonium salt.

## 4.4. Product analysis of thermal decomposition of oxoammonium salt

### 4.4.1. Identification of the major reaction product

In the investigation of TEMPO decay at high temperature, the fate of oxoammonium salt is crucial as its decomposition is the main side reaction. To determine the mechanism of oxoammonium salt decomposition, the reaction product was studied by NMR spectroscopy. Surprisingly, ^{13}C-NMR spectrum of the reaction mixture was unexpectedly noisy, although no paramagnetic species can be detected from its EPR spectrum. This effect significantly interferes with our investigation.

#### 4.4.1.1. Fast electron transfer between TEMPO and oxoammonium cation

The fast electron hopping between TEMPO and oxoammonium cation can explain the lack of signal in the $^{13}$C NMR spectra. There is only one electron difference between TEMPO and oxoammonium cation. The fast electron exchange reaction between these two structures (Scheme 4.6) significantly broadens both NMR and EPR spectra, leading to signal broadening beyond detection[6].
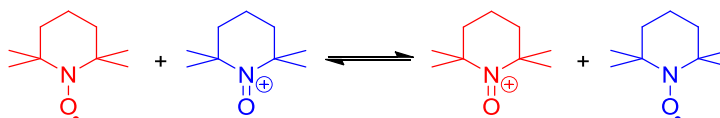


**Scheme 4. 6. Electron self-exchange between TEMPO and oxoammonium cation.**

This effect is demonstrated by studying EPR signal intensity of different concentration of oxoammonium chloride. Pure oxoammonium cation is EPR silent. The presence of a small amount of TEMPO as impurity results in an EPR signal which is observed in dilute oxoammonium salt aqueous solutions. However, at high concentration of oxoammonium cation, the broadening as a result of the electron exchange is significant, which makes the solution EPR silent. Figure 4.11 shows EPR spectra of different concentrations of oxoammonium chloride in the aqueous solutions. At low concentration of oxoammonium salt, EPR signal of TEMPO is strong. As oxoammonium salt concentration increases, EPR signal of TEMPO drops significantly, and eventually becomes invisible at 10000 ppm oxoammonium chloride.
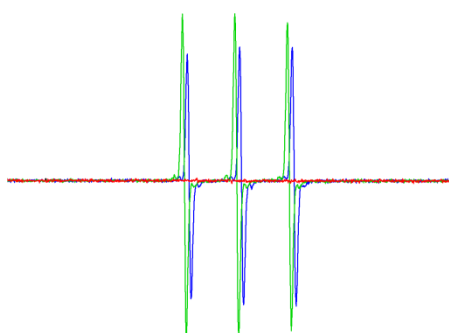


**Figure 4. 11. Different concentration of oxoammonium chloride in water. Red: 10000ppm. Blue: 1000ppm. Green: 500ppm.**

Similarly, the electron exchange between TEMPO impurity and oxoammonium salt also broadens $^{13}$C NMR spectra beyond detection. Therefore, a reducing agent (e.g.

phenylhydrazine) is often introduced into the reaction mixture to reduce TEMPO and oxoammonium salt to hydroxylamine and thus obtain structural information.

### 4.4.1.2. Identification of hydroxylamine as the major reaction product of thermal decomposition of oxoammonium salt

Phenylhydrazine is commonly used to reduce nitroxide radicals to hydroxylamine *in situ* to obtain structural information from NMR spectroscopy[7]. Therefore, in order to identify the reaction product, a solution of 1% (w/w) TEMPO in 1 M $H_2SO_4$ in $D_2O$ was heated at 80 °C for 24 hours. Aliquots of the reaction mixture were taken and reduced by excess phenylhydrazine. The reduced samples were analyzed by ^{1}H and ^{13}C NMR spectroscopy. As shown in Figure 4.12, both ^{1}H and ^{13}C NMR suggested that major product after reduction was TEMPO hydroxylamine.
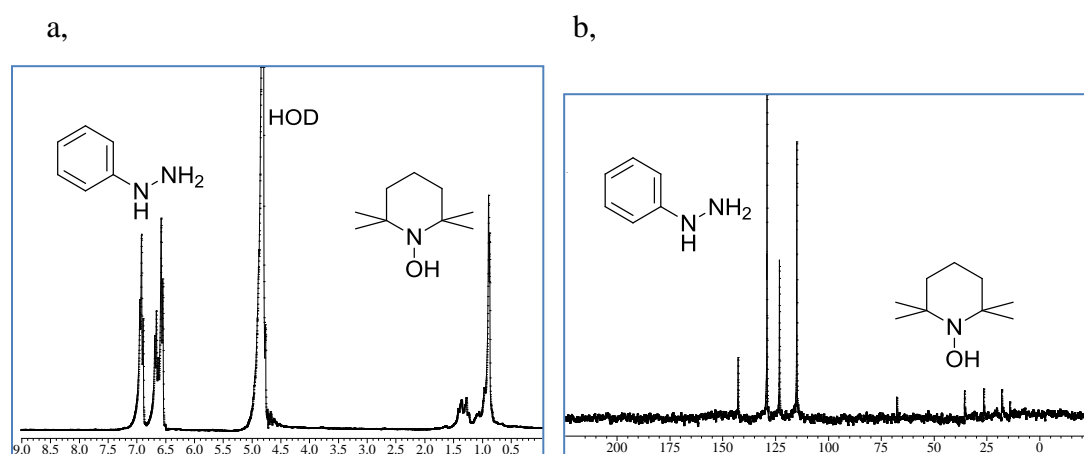
a,                                                    b,



**Figure 4. 12. NMR spectra of 1% (w/w) TEMPO in 1M $H_2SO_4$ heated at 80 °C for 24 hours, reduced by PhNHNH$_2$. a, [1]H. b, [13]C.**

The NMR spectra of the reaction mixture match the spectra of TEMPO hydroxylamine in sulphuric acid (Figure 4.13). This suggests TEMPOH is a major product in the reaction mixture. In order to confirm the stability of TEMPOH at the same condition, a solution of TEMPOH in 1M $H_2SO_4$ in $D_2O$ was heated at 80 °C for 23 hours. No change was observed in the NMR spectra. This suggests that TEMPOH is thermally stable at 80 °C in acid. The germinal methyl groups of TEMPOH are not equivalent, which can be observed from the ^{13}C NMR spectrum, and in some cases, from the ^{1}H NMR spectrum as well.
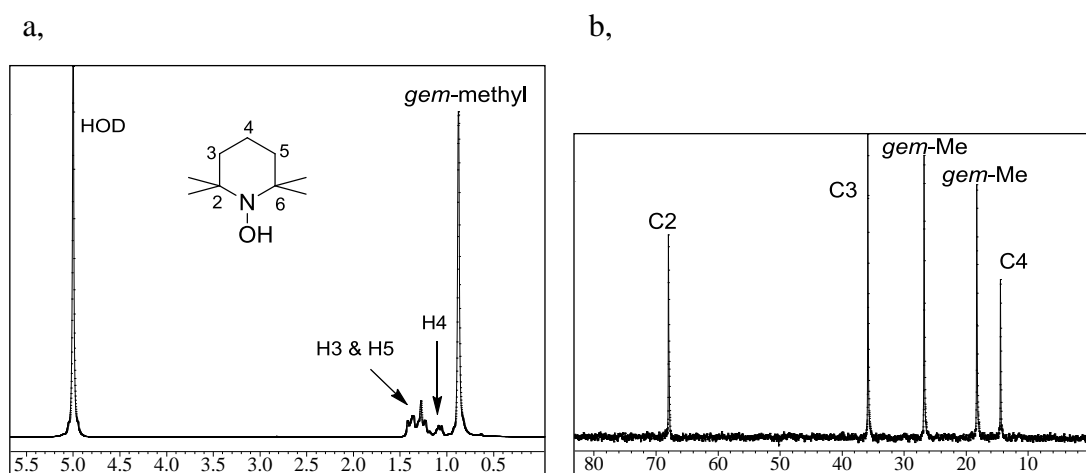
a,

b,



**Figure 4. 13. NMR spectra of TEMPOH in 1M $H_2SO_4$ in $D_2O$. a, $^1H$ NMR. b, $^{13}C$ NMR.**

A quantitative analysis was then carried out. Phenylhydrazine was used not only as a reductant but also as an internal standard. As shown in Table 4.1, the integration of phenylhydrazine peak is preset to 5.0 and 2.0, respectively, according to the amount of phenylhydrazine (50 mg and 20 mg, respectively) used for reduction. Thus the intensity of TEMPO hydroxylamine (TEMPOH) peaks is a measure of the amount of hydroxylamine present in the reaction mixture. The integration of geminal methyl groups of TEMPOH dropped from 2.9 to 2.4 after heating for 24 hours, which suggest *ca.* 17% loss of TEMPOH after the reaction mixture was heated.

**Table 4. 1. Quantitative $^1H$ NMR product analysis of TEMPO in 1M $H_2SO_4$, before and after the reaction at 80 ℃. Phenylhydrazine was used as an internal reference and reductant of the radicals.**

|  | δ/ppm | Assignment | Integration |
|---|---|---|---|
| Before heating[a] | 6.9-7.1 | 3,5-proton of $PhNHNH_2$ | 5.0 |
|  | 0.8-1.1 | *gem*-$CH_3$ of TEMPOH | 2.9 |
| After heating[b] | 6.8-7.1 | 3,5-proton of $PhNHNH_2$ | 2.0 |
|  | 0.8-1.1 | *gem*-$CH_3$ of TEMPOH | 2.4 |

a, A 0.7mL solution of 10mg/mL TEMPO in 1M $H_2SO_4$ in $D_2O$ was reduced by **50** mg $PhNHNH_2$ immediately after preparation. b, Reaction mixture was heated at 80 ℃ for 24h, and then 0.7mL solution was reduced by **20** mg $PhNHNH_2$.

TEMPOH observed after reduction of the reaction mixture could either be TEMPOH in the product or TEMPO which is reduced by phenylhydrazine. Hence, in order to

determine which one is the product, the crude reaction mixture was oxidized to examine if EPR signal of TEMPO will increase. Tungstate catalyzed oxidation of hydroxylamines by hydrogen peroxide leads to the corresponding nitroxide radicals. (Scheme 4.7).[8]

$$2 \, \text{>N-OH} \ + \ H_2O_2 \ \xrightarrow{\text{WO}_4^{2-}} \ 2 \, \text{>N-O}^{\bullet} \ + \ 4H_2O \ + \ O_2$$
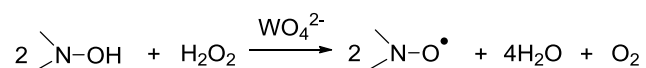
**Scheme 4. 7. Tungstate catalyzed oxidation of hydroxylamine to nitroxide radical by hydrogen peroxide.**

An aqueous solution of 10mg/mL (0.052 M) oxoammonium chloride was heated at 80°C for 6 hours to allow oxoammonium salt to completely decompose (as monitored by UV spectroscopy). Then the reaction mixture was oxidized with a 10-fold excess of 30% $H_2O_2$ in the presence of a catalytical amount of $WO_4^{2-}$ at room temperature over 10 hours. A significant increase of TEMPO intensity was observed by EPR (Figure 4.14), which suggests the presence of large amount of hydroxylamine in the reaction mixture. Assessing from the double integration of the EPR spectra as compared to the initial concentration, the oxidation product accounted for 54% (molar fraction) of the starting material.
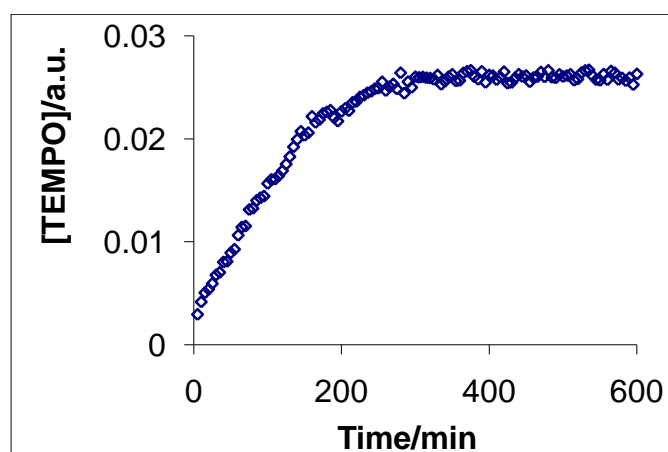


**Figure 4. 14. Oxidation of oxoammonium chloride decay in $H_2SO_4$ reaction mixture by 10-fold excess 30% $H_2O_2$ in the presence of $WO_4^{2-}$. The solution of 0.052 M oxoammonium chloride in 1M $H_2SO_4$ was heated at 80°C for 6 hrs prior to oxidation.**

Both reduction and oxidation of oxoammonium salt mixture thus suggest that the main product of thermal decomposition of oxoammonium chloride is hydroxylamine

(Scheme 4.8). Hence, this reaction is a reduction of oxoammonium salt to hydroxylamine. The oxidation product of the reaction is not identified.
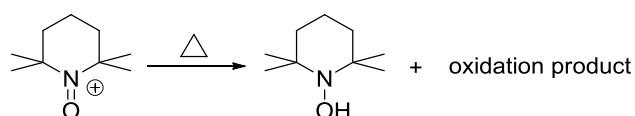


**Scheme 4. 8. Thermal decomposition of oxoammonium cation.**

## 4.4.2. Quantification of the yield of hydroxylamine

Hydroxylamine has been identified as a major product in thermal decomposition of oxoammonium salt. As shown in Table 4.1 (p159), the quantitative study showed that after heating an aqueous solution of TEMPO at 80 ℃ for 24 hours, the yield of hydroxylamine is *ca.* 83%. Only 17% TEMPO forms other reaction products (e.g. ring opening products).

The accuracy of the quantitative NMR study was limited due to presence of radicals in the system. Even after reduction with a tenfold excess of phenylhydrazine, EPR signal of nitroxide radicals is still detectable. To confirm the result of the quantitative NMR study, an alternative agent can be used to reduce nitroxide radicals in order to rule out the effect of the reducing agent. Hence, the quantitative experiment was repeated using sodium *L*-ascorbate (Na-ASC) as a reductant and the internal reference. A $D_2O$ solution of 10 mg/mL TEMPO in 1 M $H_2SO_4$ was heated at 80 ℃. Aliquots of the reaction mixture was taken at different reaction times and reduced by excess sodium L-ascorbate. The NMR spectra were analyzed quantitatively by comparing the integration of the gem-methyl groups of hydroxylamine and the methylene group of ascorbate. The result is shown in Table 4.2. The amount of sodium ascorbate used for reduction is consistent amongst different reaction times. Thus the integration of gem-methyl groups of TEMPOH signal is a measure of the amount of TEMPOH in the reduced reaction mixture.

**Table 4. 2.** $^1$H NMR of 10mg/mL TEMPO in 1M $H_2SO_4$ in $D_2O$ at 80 ℃ for different reaction time. Solution was reduced by sodium L-ascorbate. Using ascrobate as reference, the amount of TEMPO only changed slightly before and after heating.

| Reaction time | Signal($\delta$/ppm) | Assignment | Integration |
|---|---|---|---|
| 0 | 3.5 | Na-ASC $CH_2$ | 1.0 |
| | 0.9-1.1 | TEMPOH gem-Me | 1.6 |
| 2.5h | 3.5 | Na-ASC $CH_2$ | 1.0 |
| | 0.9-1.1 | TEMPOH gem-Me | 1.4 |
| 9h | 3.5 | Na-ASC $CH_2$ | 1.0 |
| | 0.9-1.1 | TEMPOH gem-Me | 1.3 |
| 24h | 3.5 | Na-ASC $CH_2$ | 1.0 |
| | 0.9-1.1 | TEMPOH gem-Me | 1.3 |

Similarly, after reaction at 80 ℃ for 24 hours, only 19% of TEMPO forms other reaction products. This result is consistent with previous quantitative analysis discussed in Section 4.4.1.2 (p158). Due to the presence of radicals (e.g. TEMPO) in the reaction mixture even after reduction reactions, the yield obtained may not be perfectly accurate. However, the effect of radicals can be assumed to be similar throughout the study, therefore can be considered as systematic error. Hence, the quantitative study of the product was proved to be reproducible.

The same method was used to quantify the yield of hydroxylamine directly from oxoammonium salt decomposition. A solution of 4% oxoammonium chloride in 1 M $H_2SO_4$ in $D_2O$ was heated at 80 ℃. At different reaction times aliquots of the reaction mixture were taken. The samples were reduced by excess phenylhydrazine and analyzed by $^1$H and $^{13}$C NMR spectroscopy (Figure 4.15).
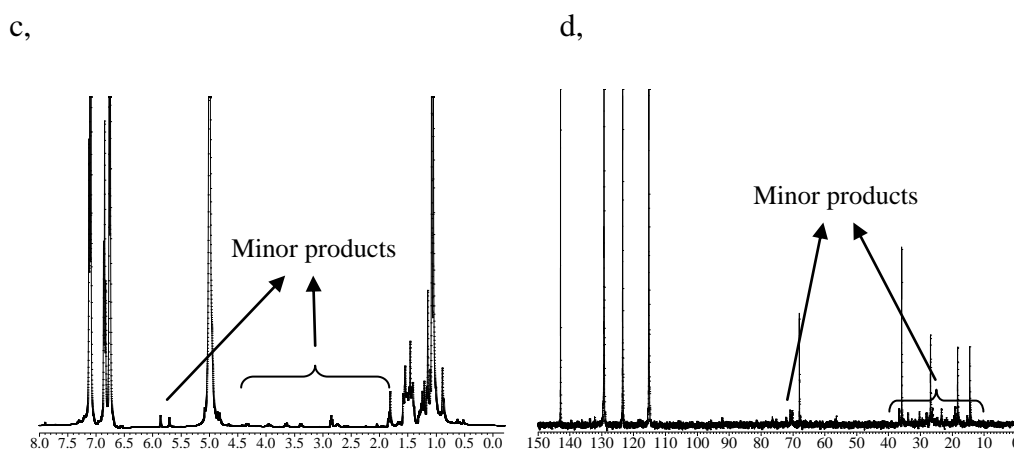
a,                                              b,

c,                                                    d,
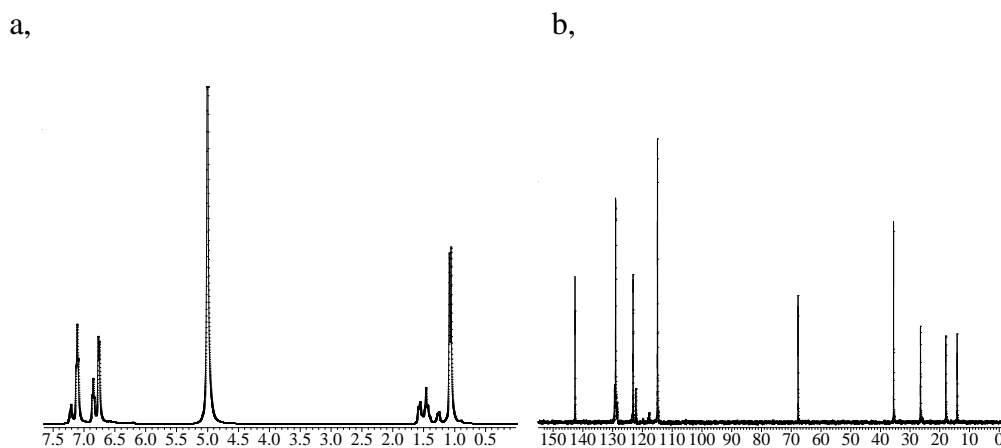


**Figure 4. 15. NMR spectra of reaction mixture of 4% oxoammonium chloride in 1 M $H_2SO_4$ in $D_2O$ at 80 °C, after reduction by $PhNHNH_2$. a, $^1H$ NMR spectrum of the reaction mixture before heating. b, $^{13}C$ NMR spectrum of the reaction mixture before heating. c, $^1H$ NMR spectrum of the reaction mixture after heating for 2 hrs. d, $^{13}C$ NMR spectrum of the reaction mixture after heating for 2 hrs.**

Minor amount of side reaction product was already observed (as highlighted in Figure 4.15c-d) after the reaction carried out for 2 hours. Unfortunately, the side reaction products also give a methyl signal which overlaps with the germinal methyl groups of hydroxylamine. It may not have a significant impact on the quantitative analysis if the amount of such products is small. Hence, the yield of hydroxylamine was also quantified from this experiment, which gives a yield of 64% after reacted for 5 hours.

An attempt was also made to separate the side reaction product by extracting it from the aqueous reaction mixture to $CDCl_3$. TEMPOH is protonated in sulphuric acid therefore stays in the aqueous phase. Some side reaction product was extracted and analyzed by NMR spectroscopy (Figure 4.16).
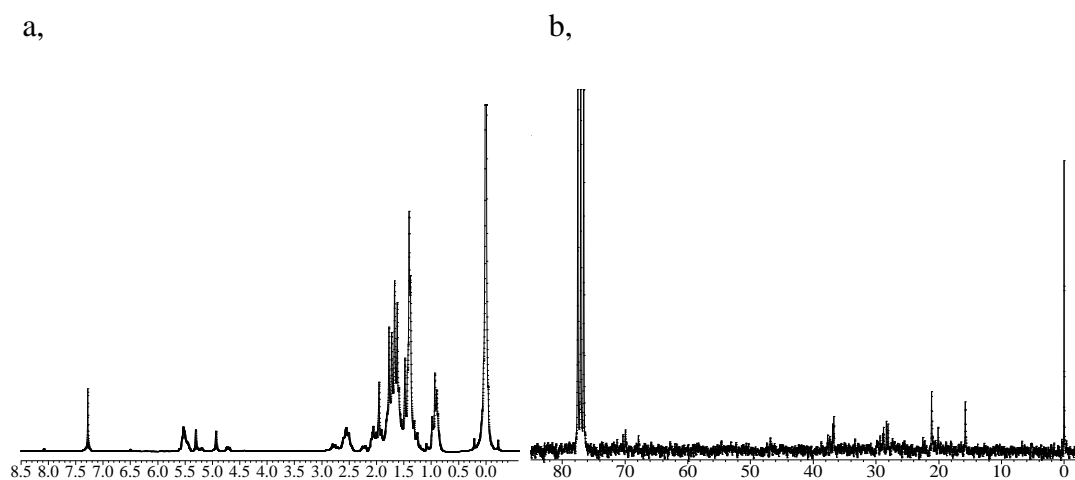
a,                                              b,



**Figure 4. 16. NMR spectra of the reaction mixture extracted by CDCl₃. The reaction was 4% oxoammonium chloride in 1 M H₂SO₄ in D₂O at 80 ℃ for 111 hours. a, ¹H NMR spectrum. b, ¹³C NMR spectrum.**

As shown in Figure 4.16, in the ¹H NMR spectrum, signals at *ca.* 5-5.5ppm suggest formation of alkenes in a small amount. The ¹³C NMR spectrum has signals at positions very close to TEMPOH. As compared to the spectra of the reaction mixture (Figure 4.15), the compound may be the products of reaction at the NO group or the 4-position of oxoammonium salt. The structure, however, cannot be determined based on this information. Due to the small amount of this product, isolation of this compound by flash column chromatography was not successful.

With confirmation that the main product in the reaction mixture is TEMPO hydroxylamine, it is possible to hypothesize some reaction mechanisms. As stated in Scheme 4.3 (p145), oxidation of H₂O by oxoammonium salt was proposed. This mechanism could explain the high yield (*ca.* 64%) of hydroxylamine from thermal decomposition of oxoammonium salt. Hydrolysis of oxoammonium cation would lead to formation of hydroxyl radical and TEMPO. In acid, TEMPO would disproportionate to form additional hydroxylamine and oxoammonium salt. As a result, this mechanism would lead to accumulation of hydroxylamine in the product.

The other possible mechanism considered for the reaction is via a ring-opening process (Scheme 4.9).
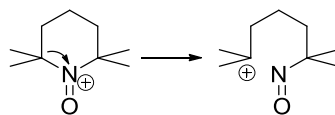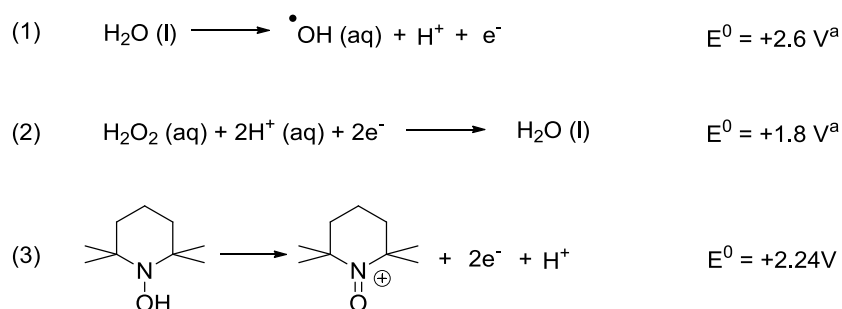
**Scheme 4. 9. Ring opening reaction of oxoammonium cation.**

The carbocation product of the ring-opening mechanism can form an alkene and further eliminate to give dienes. It is also possible to form nitroso compounds via spin trapping methanisms. These possible mechanisms are discussed in detail in the next section.

## 4.5.    The mechanism of oxoammonium salt decomposition

### 4.5.1.  Hydrolysis mechanism

The hydrolysis mechanism is shown in Scheme 4.3 (p145), in which oxoammonium cation is hydrolyzed and eventually leads to accumulation of hydroxylamine. This mechanism can thus explain the high yield of hydroxylamine. However, many observations cannot be explained by this mechanism. Firstly, oxoammonium salt decomposition was also observed in anhydrous conditions (e.g. distilled acrylic acid). It suggests that thermal decomposition of oxoammonium salt does not depend on $H_2O$. Secondly, the redox potentials of reaction 1[9] and reaction 3[10] (Scheme 4.10) suggest that oxidation of water to hydroxyl radical by oxoammonium cation is physically impossible. Therefore, this reaction mechanism is ruled out. Oxidation of water to hydrogen peroxide is possible, however, we failed to detect any $H_2O_2$ in the system.

(1)  $H_2O$ (l) $\longrightarrow$ $^{\bullet}OH$ (aq) $+ H^+ + e^-$        $E^0 = +2.6\ V^a$

(2)  $H_2O_2$ (aq) $+ 2H^+$ (aq) $+ 2e^- \longrightarrow$ $H_2O$ (l)        $E^0 = +1.8\ V^a$

(3)  [structure: 2,2,6,6-tetramethylpiperidine N-OH] $\longrightarrow$ [structure: oxoammonium N$^{\oplus}$-O] $+ 2e^- + H^+$        $E^0 = +2.24V$

**Scheme 4. 10. Oxidation potential of one electron oxidation of $H_2O$ and TEMPO. a, measured at pH=0.**

## 4.5.2.  Ring opening mechanism

The second reaction mechanism we considered is a ring-opening mechanism (Scheme 4.9, p165). Many details in the mechanistic investigation suggest that oxoammonium salt decomposition may be a ring-opening process.

### 4.5.2.1.  Detection of possible ring opening product by EPR spectroscopy

As shown in Figure 4.10 (p155), UV spectra suggest that one reaction product has a UV absorbance band at *ca.* 670 nm. This product may be a nitroso-compound. Possible ring-opening reaction product was also detected by EPR spectroscopy in the decay of TEMPO in acid at high temperature (Figure 4.17). A $D_2O$ solution of 10 mg/mL TEMPO in 1 M $H_2SO_4$ was heated at 80 ℃ for 2 days and neutralized with excess $NaHCO_3$. The EPR spectrum obtained shows two components with different intensity.
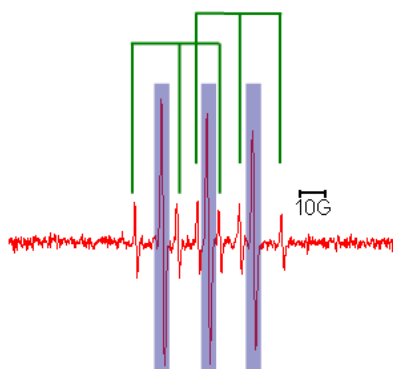


**Figure 4. 17. EPR spectrum of 10mg/mL TEMPO in 1 M $H_2SO_4$ ($D_2O$) reaction mixture, after neutralization with excess $NaHCO_3$. The solution was heated to 80 ℃ for 2 days before**

**neutralization. Hyperfine values of the 6-line component (as shown with green lines) are: $a_N$=16G, $a_H$=24G.**

The first component in Figure 4.17 is TEMPO (shown with blue bars), which is formed from comproportionation of hydroxylamine and oxoammonium salt or hydroxylamine oxidation. The second component is a doublet of triplets. The nitrogen and hydrogen hyperfine values of this component are 16 G and 24 G, respectively. The hyperfine values are consistent with a spin adduct of a common spin trap 2-methyl-2-nitrosopropane (MNP)[11], which suggests a unique structure with only one α-H atom (Figure 4.18).
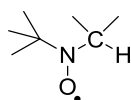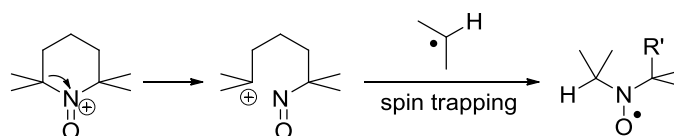


**Figure 4. 18. A typical structure of nitroxide radical with hyperfine values of $a_N$=16G and $a_H$=24G.**

The formation of such structure suggests the ring opening reaction. A nitroso compound is formed following ring opening, which could trap a secondary alkyl radical in the system to form a new nitroxide radical with one α-H atom (Scheme 4.11).



**Scheme 4. 11. Spin trapping of a reactive radical by the ring opening reaction product of oxoammonium salt.**

### 4.5.2.2. Detection of $NO_3^-$ in the reaction product

The nitroso derivatives are likely to be oxidized further. Interestingly, nitrate ($NO_3^-$) was detected in the reaction mixture using Ion Chromatography (IC). An aqueous solution of 40 mg/mL oxoammonium chloride was heated to 80 °C for 4 hours. Compared to unheated sample, the amount of nitrate is increased tenfold (Table 4.3).

**Table 4. 3. Concentraton of $NO_3^-$ detected by IC in aqueous solution of 40 mg/mL oxoammonium chloride.**

| Sample | Concentration/ppm |
| --- | --- |
| Ambient | 22 |
| 80 ℃ | 238 |

This is strong evidence that nitric acid was formed in the reaction mixture. Although the yield of nitrate is low (*ca.* 4%), the presence of $NO_3^-$ proves the ring-opening mechanism. Formation of nitrate is likely to result from elimination of the NO group from oxoammonium salt following ring opening. In order to explore possible reaction mechanism, next section considers ring-opening of 4-oxo-TEMPO.
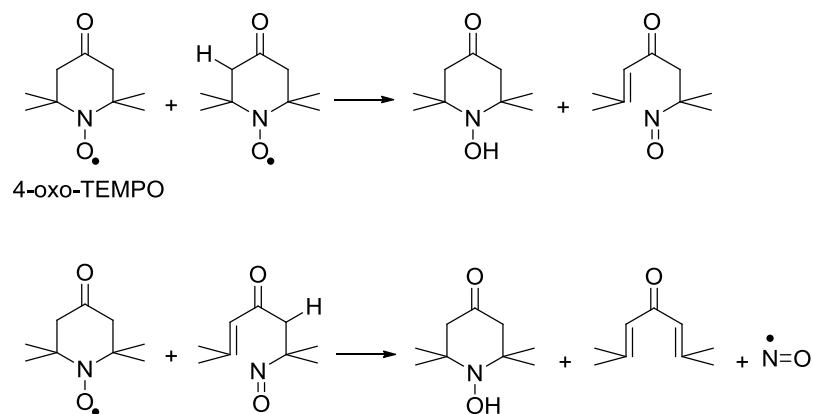
### 4.5.2.3. Ring-opening decomposition of 4-oxo-TEMPO

A ring-opening mechanism was proposed for 4-oxo-TEMPO (4OT) decomposition in 1969.[12] 4OT has a 4-keto group therefore keto-enol tautomerism makes the 3- and 5-hydrogen atoms more reactive (Scheme 4.12).
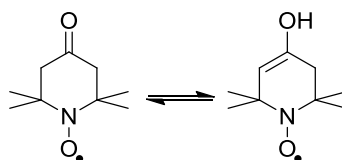


**Scheme 4. 12. Keto-enol tautomerism of 4-oxo-TEMPO.**

The proposed mechanism suggests that a molecule of 4OT can abstract an α–hydrogen of the ketone in another molecule of 4OT, to give hydroxylamine and a reactive alkene. The alkene can further react with 4OT to give hydroxylamine, the corresponding diene and NO (Scheme 4.13).

**Scheme 4. 13. Ring-opening decomposition mechanism of 4-oxo-TEMPO.**

This mechanism involves formation of NO. If a similar reaction route takes place in the TEMPO oxoammonium salt decomposition, formation of NO would explain presence of nitrate in the reaction mixture, because oxidation of NO by oxoammonium salt could lead to nitrate and hydroxylamine.

In the decay of 4-hydroxy-TEMPO (4-HT) in acid at *ca.* 100 °C, disproportionation of 4-HT leads to formation of 4-HT oxoammonium cation. The oxoammonium cation can subsequently oxidize 4-HT to 4OT (Scheme 4.14).
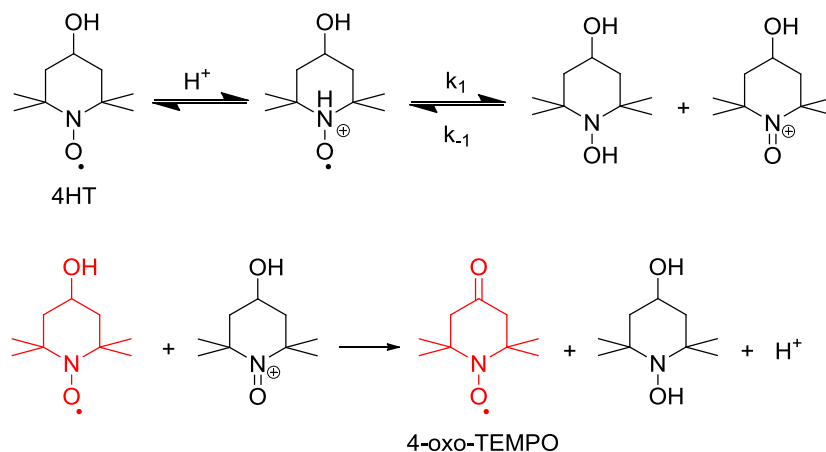


**Scheme 4. 14. Acid catalyzed 4-HT disproportionation and oxidation of 4-HT to 4-oxo-TEMPO by N-oxoammonium cation**

Therefore the mechanism shown in Scheme 4.13 is a plausible explanation of 4HT decay in acid at high temperature (e.g. 100 °C).

In the decay of TEMPO oxoammonium salt, a lack of functional group at the 4-position indicates that 3- and 5-hydrogen atoms are much more difficult to abstract. Hydrogen abstraction between TEMPO molecules was found at very high temperature (e.g. above 230 ℃). At lower temperature, this reaction is much slower.

Hence, the mechanism described in this section cannot explain formation of *ca.* 60% hydroxylamine from oxoammonium salt decomposition. In summary, product analysis of the thermal decomposition of oxoammonium salt suggests a 60% yield of hydroxylamine and trace amount of unidentified materials. Various species detected in the reaction mixture indicate a ring-opening mechanism. However, reviewing the mechanistic investigation of oxoammonium salt decomposition, inadequate information was obtained to propose a full mechanism. Product analysis result, in particular, remains a mystery since nothing substantial was found apart from 60% hydroxylamine. Possibilities were considered to explain this observation. The other products may be volatile or unstable and are thereby removed from the reaction mixture. These products probably result from an oxidation reaction which involves multiple electron transfers to enable reduction of oxoammonium salt to form a large amount of hydroxylamine. Hence, to further study the mechanism of oxoammonium salt decomposition, the reaction was monitored on a large scale.

## 4.6.    Oxoammonium salt decomposition carried out on a large scale

Thermal decomposition of N-oxoammonium chloride was then studied on a multi-gram scale. At such scale, attempts to identify or even isolate the minor reaction products can be made. It is also possible that the product may be volatile. Therefore the reaction was carried out in a closed system. $1.3 \times 10^{-3}$ M aqueous solution of oxoammonium salt was heated at 100 ℃ in a flame-sealed glass tube for 30 min. An interesting observation was noticed. During heating, gas bubbles were formed at a regular rate. After heating, a thin layer of green oily substrate was found above the aqueous layer. This surprising result suggests the reaction is more complex than expected. The reaction products are present in three phases. Therefore the three phases were studied separately.

### 4.6.1. Aqueous phase

### 4.6.1.1. Analysis of the aqueous phase product by NMR spectroscopy

A $D_2O$ solution of $1.3 \times 10^{-3}$ M oxoammonium chloride was heated to 100 ℃ in a flame-sealed glass tube for 30 min, and after the reaction the aqueous layer was separated from the organic substrate. The aqueous layer was reduced by excess phenylhydrazine and analyzed by NMR spectroscopy (Figure 4.19).
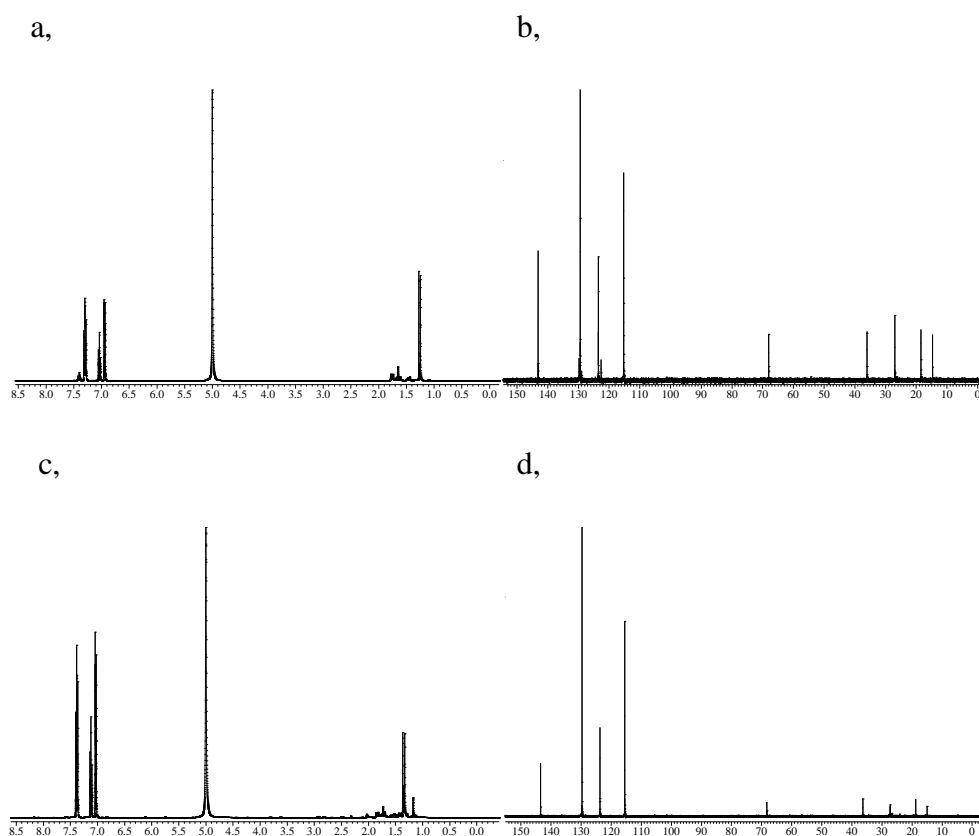


**Figure 4. 19. NMR spectra of aqueous product in $D_2O$ solution of $1.3 \times 10^{-3}$ M oxoammonium chloride heated at 100 ℃, after reduction by phenylhydrazine. a, $^1$H NMR spectrum of reduced reaction mixture before heating. b, $^{13}$C NMR spectrum of reduced reaction mixture before heating. c, $^1$H NMR spectrum of the reaction mixture heated for 30 min, after reduction by phenylhydrazine. d, $^{13}$C NMR spectrum of the reaction mixture heated for 30 min, after reduction by phenylhydrazine.**

Integration of gem-methyl groups and phenyl ring on phenylhydrazine was compared and a yield of approximately 55% was obtained. The result is consistent with the yield obtained previously.

### 4.6.1.2.        Titration of the aqueous phase product

*Titration of aqueous phase products*

The NMR studies on the aqueous phase product suggest formation of hydroxylamine. However, due to the interference of the paramagnetic species, a reduction method has to be used before NMR investigations. This could have caused further chemical reactions. In order to get a more direct quantitative analysis, the aqueous phase product was titrated using NaOH. An aqueous solution of $9.801 \times 10^{-4}$ mol oxoammonium chloride was heated to 100 °C in a flame-sealed glass tube for 30 min. After heating the oxoammonium salt solution, the green organic substrate was separated and the aqueous layer was diluted with 20 mL $H_2O$ and then titrated with 0.0207 M NaOH (aq). The pH values were monitored using a pH-meter and the titration curve was thus obtained (Figure 4.20).
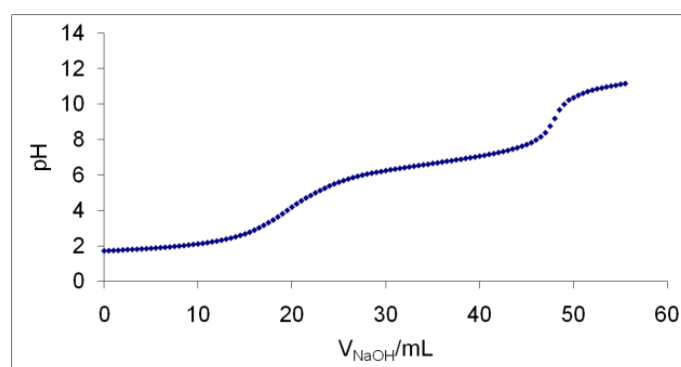


**Figure 4. 20. Titration curve of the aqueous phase product of $9.801 \times 10^{-4}$ mol oxoammonium chloride thermal decomposition at 100 °C for 30 min, titrated with 0.0207 M NaOH (aq).**

The titration curve was then analyzed (Figure 4.21). It is clear that the reaction mixture has two components (or even more). Measuring from the half equivalence points, the first component is a strong acid. The $pK_a$ obtained is below 2. The second component is a weak acid which has a $pK_a$ at around 6.6. The strong acid could be $HNO_3$ and HCl. And judging from the $pK_a$, the weak acid is probably hydroxylamine.

a,                                              b,



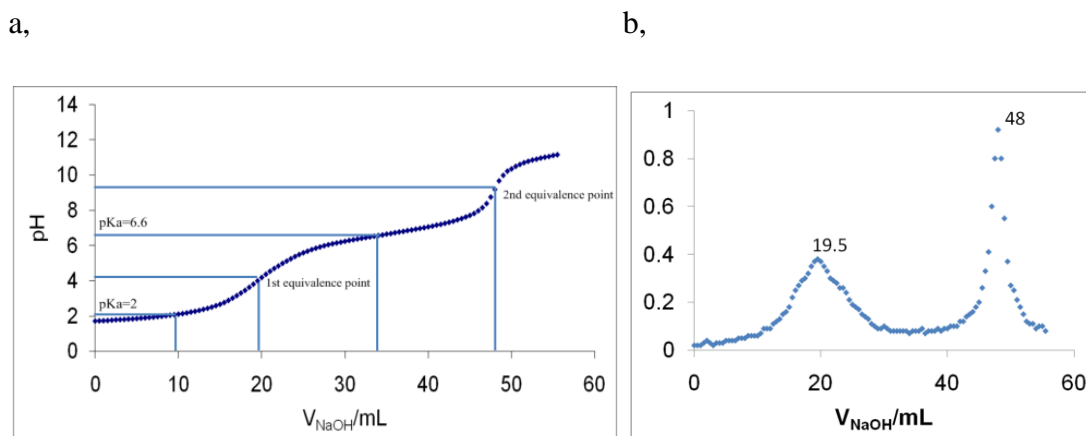**Figure 4. 21. Titration curve of the aqueous phase product of 9.801×10<sup>-4</sup> mol oxoammonium chloride decomposition at 100 ℃ for 30 min, titrated with 0.0207 M NaOH (aq). a, titration curve. b, 1<sup>st</sup>-derivative of the titration curve.**

The amount of the strong acid and weak acid was determined using the volume of NaOH used in the titration. The first equivalent (stoichiometric) point is at 19.5 mL which corresponds to the amount of NaOH used to titrate the first component. It means the amount of the strong acid is $4.04 \times 10^{-4}$ mol. Compared to the initial amount of oxoammonium salt, the yield of the strong acid is 41.2%.

Similarly, the second equivalent point was 28.50 mL. It suggests $5.90 \times 10^{-4}$ mol NaOH was used to titrate the weak acid, therefore the yield of hydroxylamine is 60.2%. Compared to the result from quantitative NMR analysis, the amount yield of hydroxylamine is consistent. The total yield of both products is 101.4%.

In order to reproduce the titration result, the experiment was repeated using a different concentration. A solution of $2.51 \times 10^{-4}$ mol oxoammonium chloride was heated at 100 ℃ in a flame-sealed glass tube for 30 min. Similarly, the aqueous phase was separated and diluted with 20 mL water. The solution was then titrated with 0.0207 M NaOH (aq). The titration curve and its first derivative are shown in Figure 4.22.
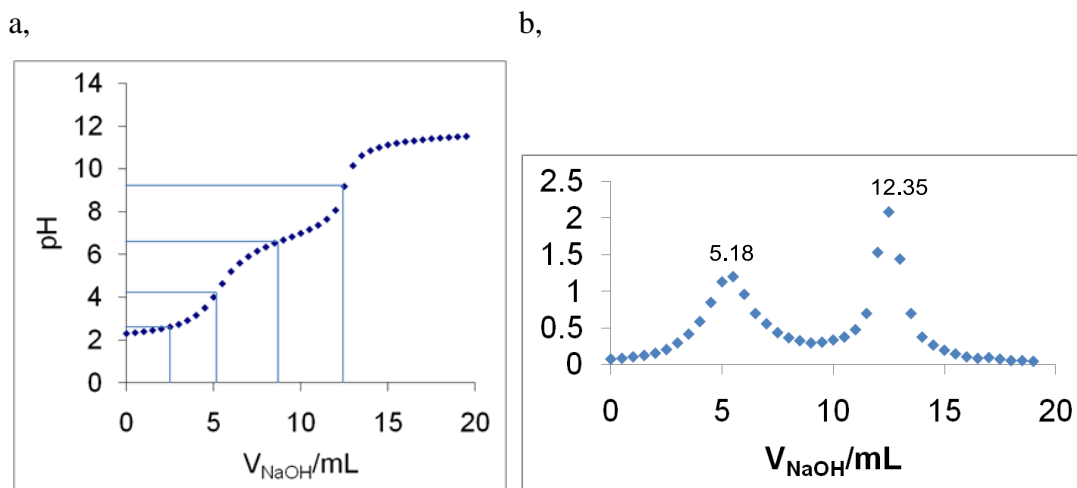
a,

b,



**Figure 4. 22. Titration curve of the aqueous phase product of $2.51 \times 10^{-4}$ mol oxoammonium chloride thermal decomposition at 100 ℃ for 30 min, titrated with 0.0207 M NaOH (aq). a, titration curve. b, 1st-derivative of the titration curve.**

Similarly, the $pK_a$ values were obtained half equivalent points. The strong acid has a $pK_a$ of below 2 and the $pK_a$ of the weak acid is 6.6. Yield of both components was determined by the amount of titrant used. This gives a yield of 42.7% for the strong acid, 59.1% for hydroxylamine and a total yield of 101.8%. This is also in good agreement with the first titration.

*Titration of hydroxylamine*

Titration of the reaction products suggests that in the aqueous phase, the main components are hydroxylamine and a strong acid. The yield of hydroxylamine is *ca.* 60%. In order to confirm the result, a solution of hydroxylamine in $H_2SO_4$ was titrated to compare with the titration curves of the reaction products. $0.61 \times 10^{-3}$ mol hydroxylamine was dissolved in 20 mL 0.02 M $H_2SO_4$. Then the solution was titrated with 0.0203 M NaOH (aq). The titration curve was thus obtained (Figure 4.23):
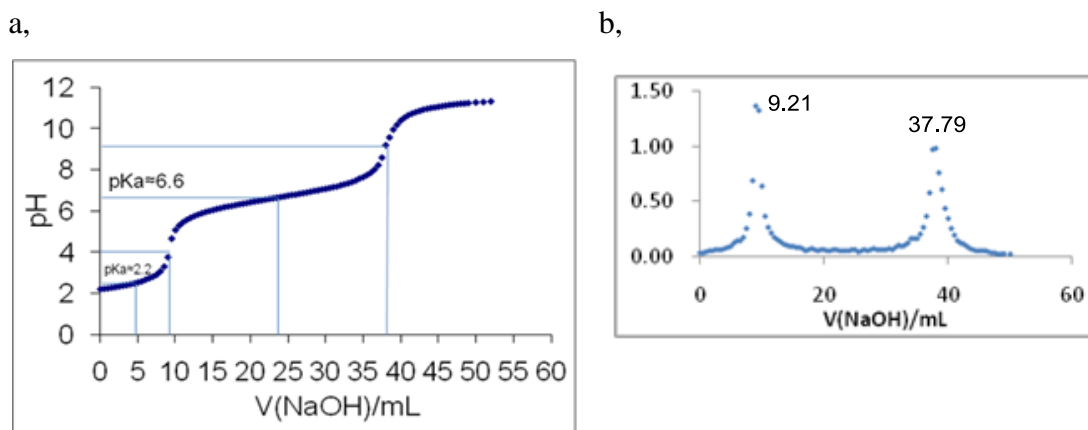
a,

b,



**Figure 4. 23. Titration curve of a solution of $0.61 \times 10^{-3}$ mol hydroxylamine in 20mL 0.02 M H$_2$SO$_4$ titrated with 0.0203 M NaOH (aq). a, titration curve. b, 1$^{st}$-derivative of the titration curve.**

As shown in Figure 4.23, the titration curve of hydroxylamine in H$_2$SO$_4$ is very similar to the titration curve of oxoammonium salt decomposition products. Two components were observed from the titration curve. The first equivalence point is 9.21 mL and the second equivalence point is 37.79 mL. The pKa values for these two components are below 2 and 6.6 which is consistent with the titration curve of the aqueous phase products of the oxoammonium salt decomposition reaction mixture. The amount of NaOH used to titrate the first component (H$_2$SO$_4$) corresponds to the excess acid in the solution. 9.21 mL NaOH was used which is equivalent to 4.61mL H$_2$SO$_4$. This means 15.39mL 0.02M H$_2$SO$_4$ was used to protonate $0.61 \times 10^{-3}$ mol hydroxylamine. It's equivalent to $0.6156 \times 10^{-3}$ mol H$^+$ was used to protonated $0.61 \times 10^{-3}$ mol hydroxylamine. The numbers match very well. 28.58 mL NaOH was used to titrate the second component (hydroxylamine). This means $0.5802 \times 10^{-3}$ mol NaOH was used to titrate $0.61 \times 10^{-3}$ mol hydroxylamine. This gives 95.2% purity of the hydroxylamine.

In summary, product analysis of the aqueous phase suggests that the major components are a strong acid, presumably HCl and TEMPO hydroxylamine. The yield of both components was determined to be *ca.* 40% for the strong acid and 60% for TEMPOH. The result confirmed that decomposition of oxoammonium salt yielded 60% TEMPOH.

### 4.6.2. Analysis of organic phase

The colour of the organic phase indicates that a nitro- or nitroso-compound may be formed, which suggests ring-opening mechanism. Besides, the hydrophobic nature of the substrate may originate from elimination of NO group from oxoammonium salt. It's difficult to determine the accurate yield of this substrate since it is volatile. The amount formed is approximately 3-4% by weight compared to the starting material. Although formed in small amount, it is not clear if the substrate has one component or more. Thereby this organic layer was extracted in trichloromethane and washed with $H_2O$. Various techniques have been applied to study the composition of the product.

### 4.6.2.1.        UV-*vis* analysis

The green colour of the organic layer probably indicates a nitrogen-containing structure. As discussed earlier (Section 4.3.4, Figure 4.10, p155), a UV active reaction mixture which has an absorbance at 670 nm was detected. It was assumed that this UV band originates from a nitro- or nitroso-compound. We also speculate that the green organic product is responsible for the UV absorbance at 670 nm. Therefore the organic layer was separated and washed with $H_2O$, then diluted in trichloromethane. A UV spectrum of the organic substrate was then obtained. As shown in Figure 4.24, a UV absorbance at *ca.* 670 nm was observed which is consistent with the previous observation. This band corresponds to an $n_N \rightarrow \pi^*$ transition. As reported, C-nitroso monomers have a UV band at this region[5]. Although the result is neither conclusive nor specific enough to determine the structure of this product, it seems plausible to assign this UV band to a C-nitroso compound.
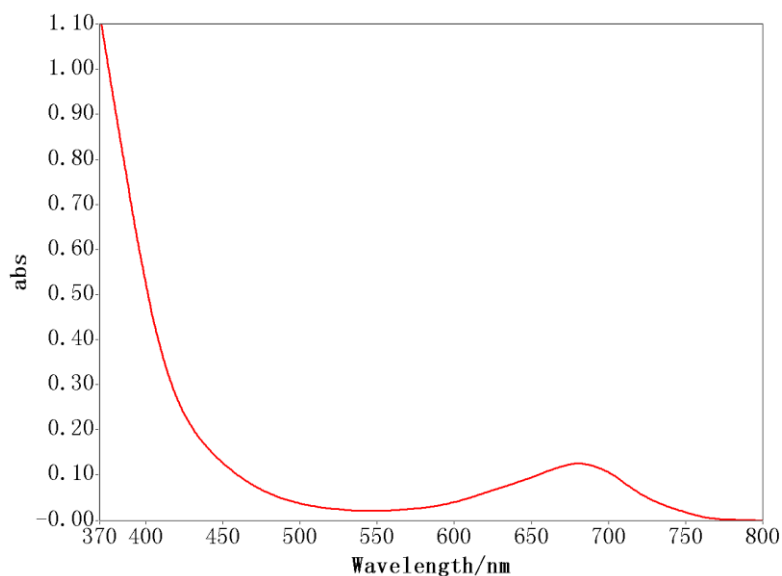
**Figure 4. 24. UV-*vis* spectrum of the green organic substrate in trichloromethane.**

### 4.6.2.2.    TLC

An attempt to isolate different components in the green substrate using Thin Layer Chromatography (TLC) was made. Among various solvent mixtures, hexane and ethyl acetate (1:1) resulted in the best separation effect, which suggested six components present in the substrate (Figure 4.25). Since the substrate is formed in a small amount and some components are not stable, isolation by Flash Column Chromatography was not possible.



In hexane/ethyl acetate (1:1)
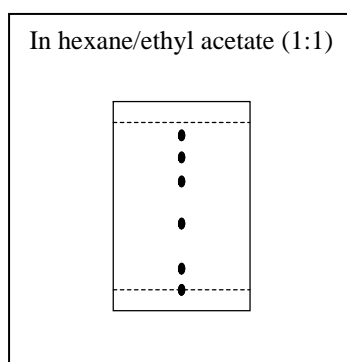
**Figure 4. 25. Separation of the green substrate in 1:1 (v/v) hexane/ethyl acetate using TLC.**

### 4.6.2.3.    GC-MS

177

Since TLC of the substrate showed multiple components, the green oily substrate was analyzed by GC-MS. The temperature program was held at 60 ℃ for 2 min, and then increased from 60 to 350 ℃ by a 5 ℃ per min increase and finally an isothermal period of 10 min at 350 ℃. The GC chromatogram (Figure 4.26) suggests that several components exist in the green oily substrate, which is consistent with the TLC findings.
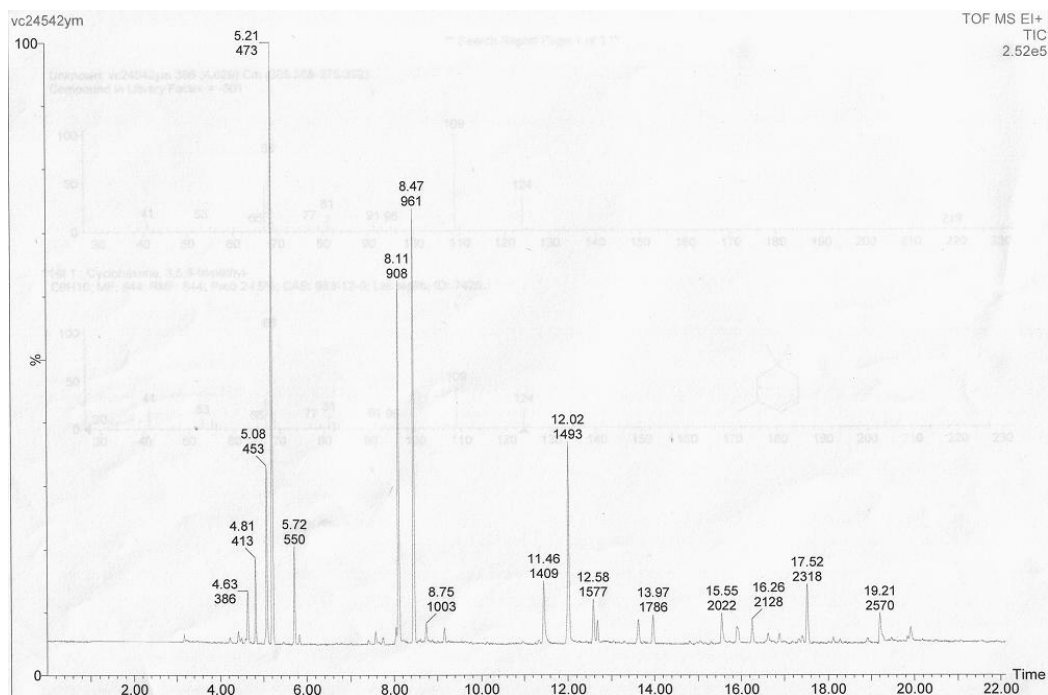


**Figure 4. 26. GC chromatogram of the green orangic substrate in trichloromethane.**

The separate peaks were analyzed by MS using electron impact (EI) ionization. The results are shown in Figure 4.27-4.34.

*1, Retention time = 4.63 min*
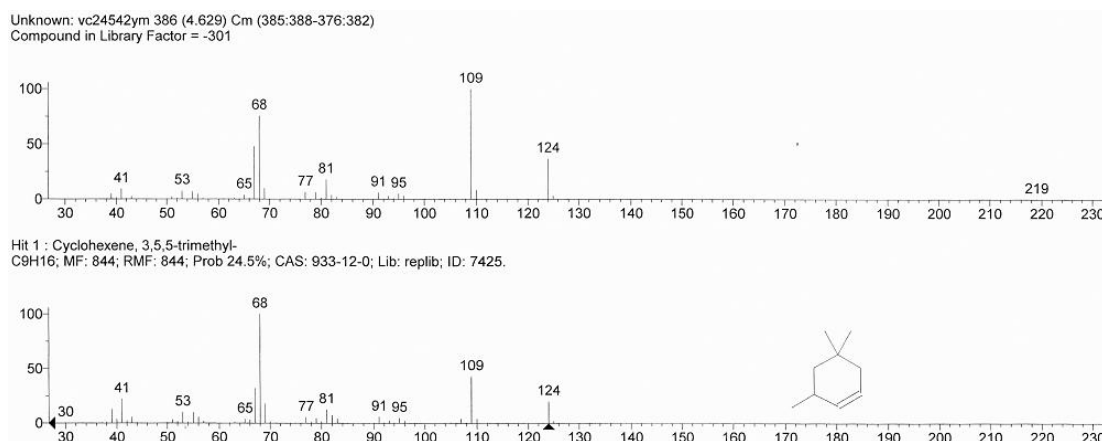


**Figure 4. 27. Mass spectra of the component at retention time 4.63 min.**

Figure 4.27 shows a relatively more volatile component. The ion at m/z=124 is likely to be the molecular ion. The ion at m/z=219 is likely to be a background peak because no fragments exists between 219 and 124. A search report shows 3,5,5-trimethylcyclohex-1-ene ($C_9H_{16}$) has a matching probability of 24.5%. Considering the pattern of the mass spectrum, a branched ring structure is possible for this compound. However, the exact structure of this compound cannot be determined from this mass spectrum.

*2, Retention time = 4.81 min*
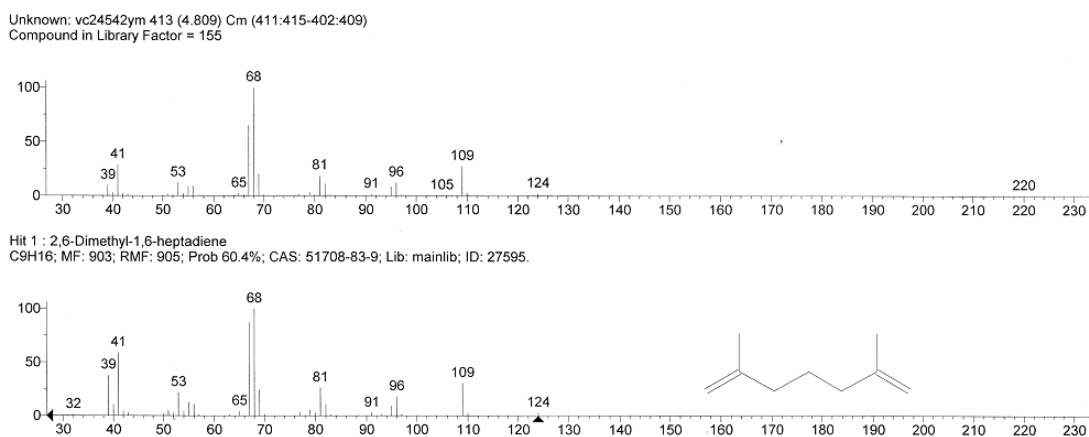


**Figure 4. 28. Mass spectra of the component at retention time 4.81 min.**

179

The component shown in Figure 4.28 has a similar boiling point with a later component which has a retention time=5.08 min. The typical hydrocarbon pattern of the mass spectrum is consistent with the structure suggested by the search report.
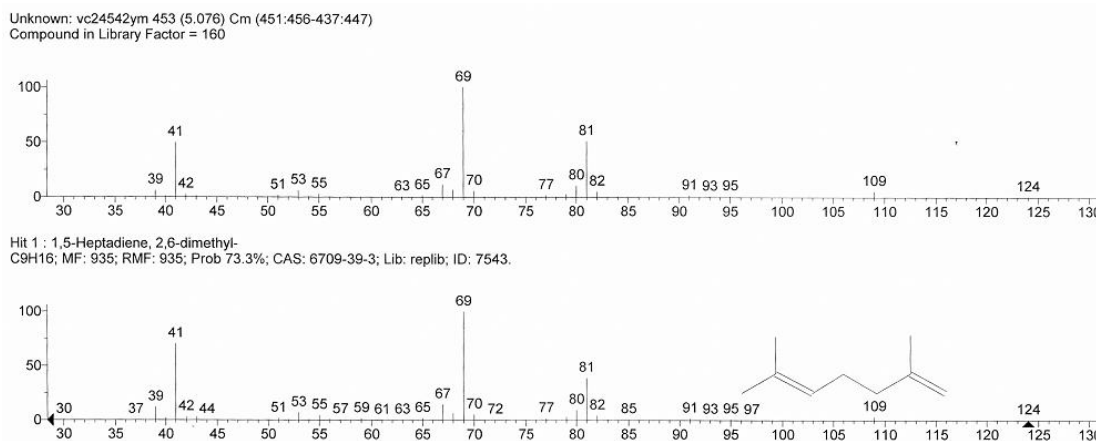
*3, Retention time = 5.08 min*



Unknown: vc24542ym 453 (5.076) Cm (451:456-437:447)
Compound in Library Factor = 160

Hit 1 : 1,5-Heptadiene, 2,6-dimethyl-
C9H16; MF: 935; RMF: 935; Prob 73.3%; CAS: 6709-39-3; Lib: replib; ID: 7543.

**Figure 4. 29. Mass spectra of the component at retention time 5.08 min.**

The two components which have the retention time of 4.81 min and 5.08 min (Figure 4.29), are likely to be two isomers of $C_9H_{16}$ diene. The matching probabilities of the given structures are 60.4% and 73.3%, respectively. Although the probability numbers are not high enough to unambiguously determine the suggested structures, the fragmentation pattern is very similar. Therefore we believe that these two components are the dienes suggested or their close isomers.
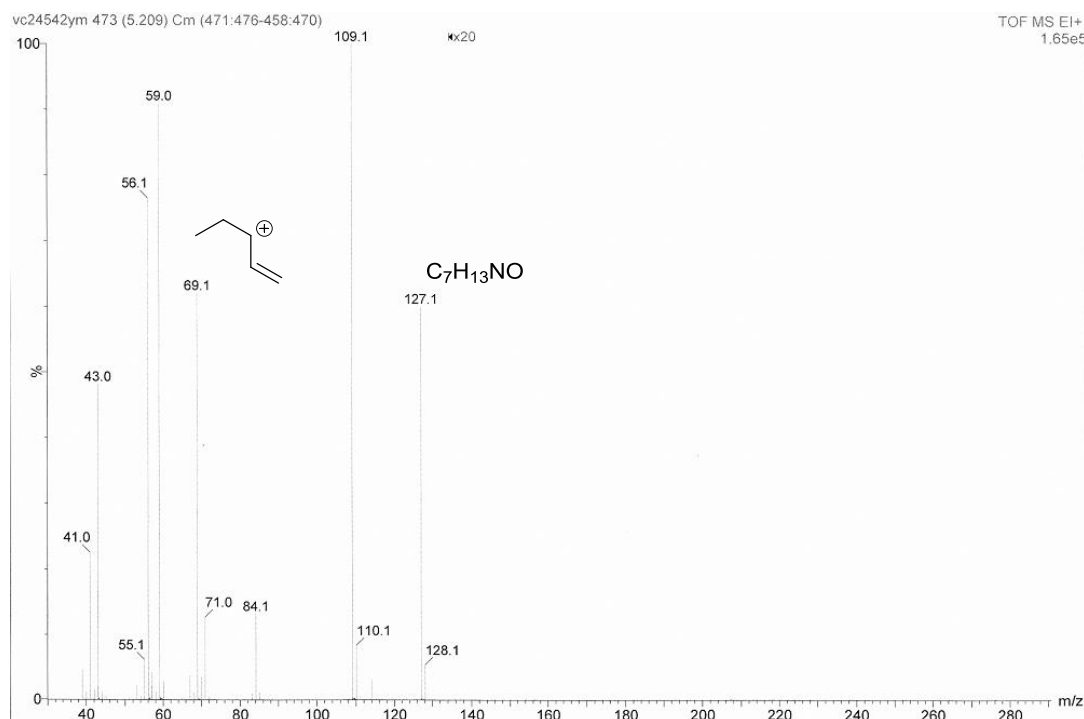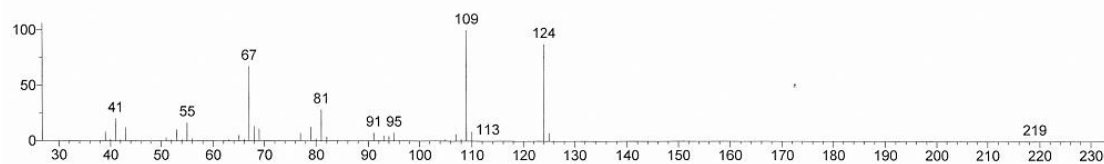
*4, Retention time = 5.21min*



**Figure 4. 30. Mass spectrum of the component at retention time 5.21 min.**

The peak at retention time = 5.21 min (Figure 4.30) is the main component in the substrate due to its intensity. The molecular ion is at m/z=127.1 considering the relative abundance of A+1=128.1. The molecular ion was thus determined to be $C_7H_{13}NO$ as it has an odd number of electrons and the ratio of its M/M+1 is consistent with the spectrum. The number of rings and double bonds in $C_7H_{13}NO$ is 2. High intensity of the molecular ion suggests the compound has a ring structure. The possible structures of this species include a 6-member-ring hydroxylamine and a 5-member-ring nitroso compound, or their isomers (Table 4.4, p185). Peaks at 69.1 and 109.1 are two fragments which were also observed in the mass spectra of other components of the GC chromatogram. The peak at 109.1 could be a nitrogen containing radical cation, with a formula of $[C_7H_{11}N]^{\bullet+}$. The peak at 59.0 is likely to be a nitrogen-containing fragment of the ring opening product, which has a formula of $[C_2H_5NO]^{\bullet+}$. The peak at 69.1 could be a further fragment of the diene, with a formula of $C_5H_9{}^+$.
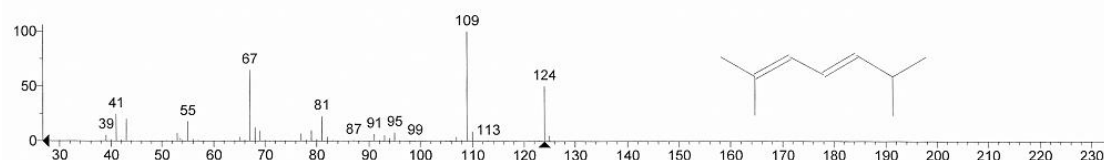
*5, Retention time = 5.72min*



**Figure 4. 31. Mass spectra of the component at retention time 5.72 min.**

The component shown in Figure 4.31 has a molecular ion at m/z=124. Matching to mass spectrum of 2,6-dimethyl-2,4-heptadiene gives a probability of 29.1%. However, the fragmentation pattern is very similar, which indicates the compound is also a diene.
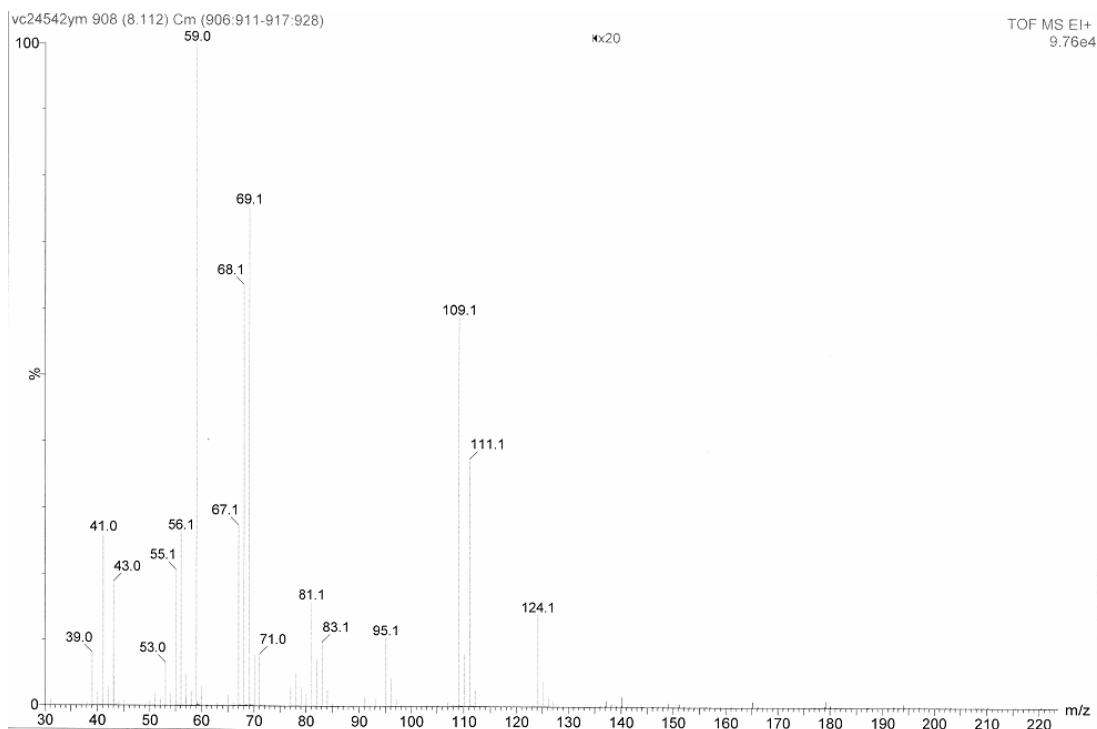
*6, Retention time = 8.11min*



**Figure 4. 32. Mass spectra of the component at retention time 8.11 min.**

The component shown in Figure 4.32 has similar retention time with a later component at 8.47 min. The two components also have similar mass spectra. It is likely that these two components are isomers which have similar structure. Therefore, the two components are discussed together.
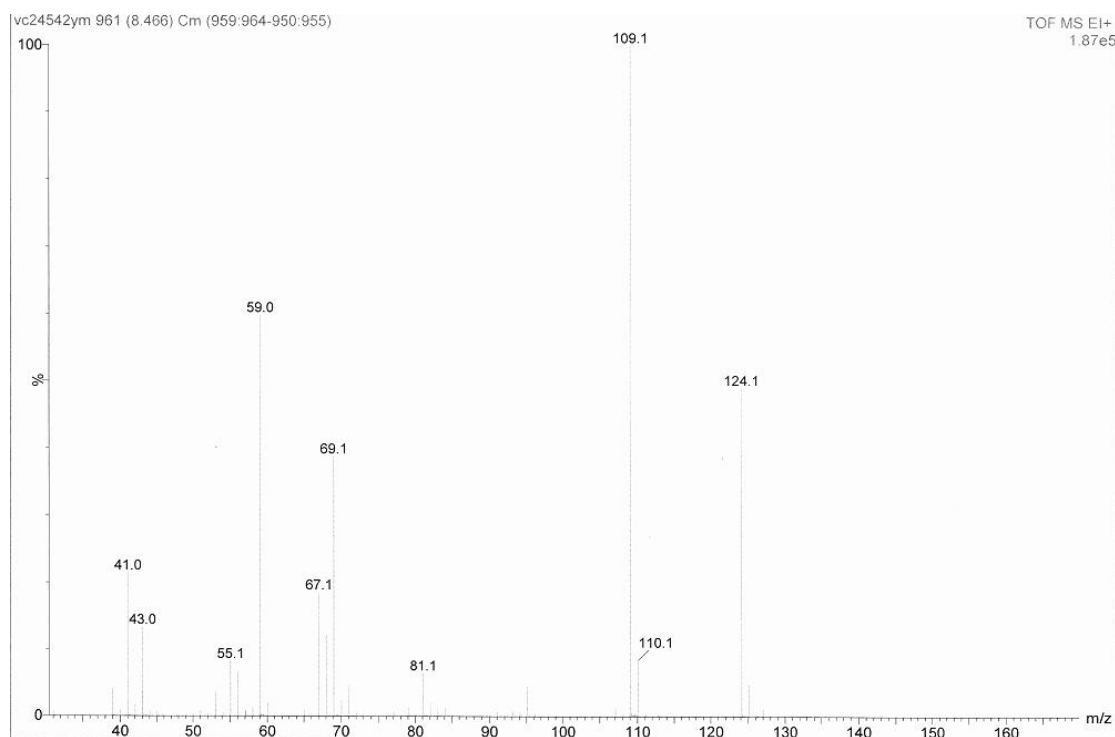
*7, Retention time = 8.47min*



**Figure 4. 33. Mass spectra of the component at retention time 8.47 min.**

The two components at retention time 8.11 min and 8.47 min (Figure 4.33) are isomers. The similar boiling points suggest they have similar structures. Since these two components have higher boiling points than the previous components (probably dienes), it is possible that these two components are $C_9H_{16}$ alkynes. However, the diene structures cannot be ruled out. The structure of these components cannot be determined.
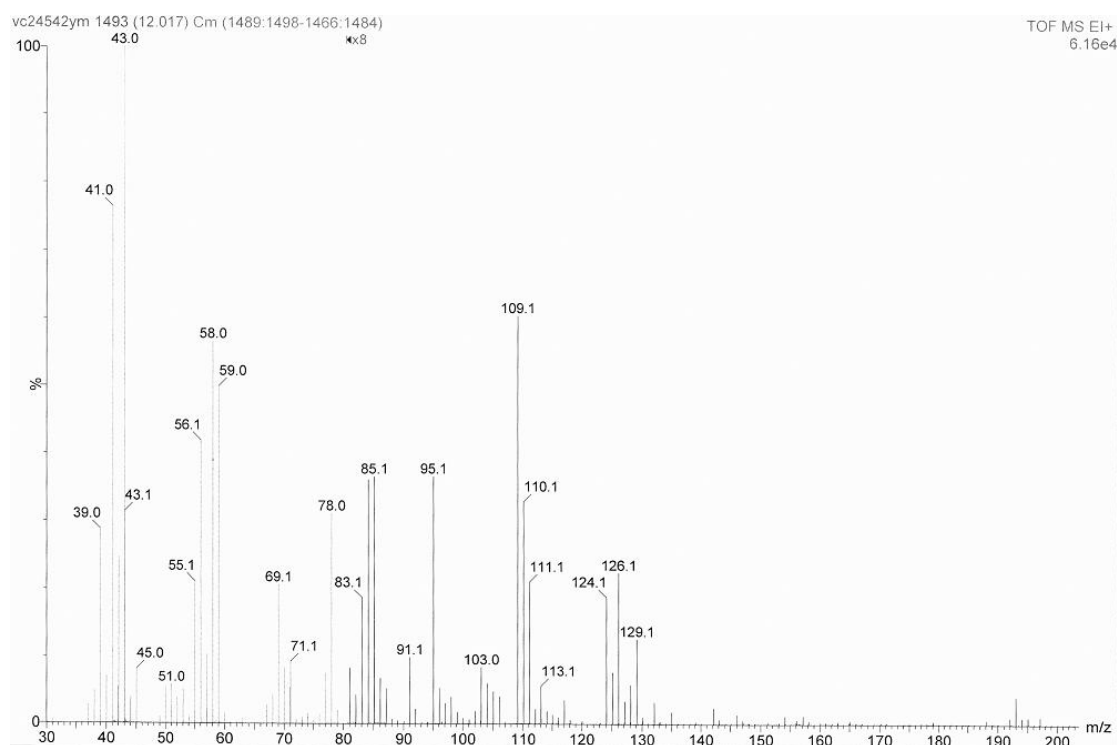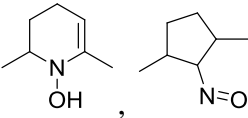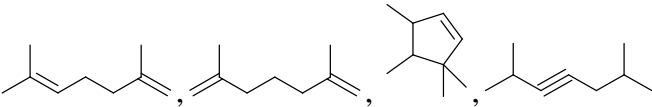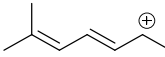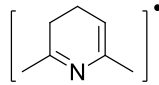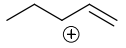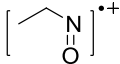
*8, Retention time = 12.017min*
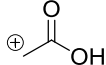


**Figure 4. 34. Mass spectra of the component at retention time 12.02min.**

The component shown in Figure 4.34 has a higher boiling point (*ca.* 20-35 ℃ higher) than previous components. The molecular ion is probably at m/z=193. It shares some ion peaks compared to the diene components (e.g. 124.1, 109.1), however, the information is not enough to propose a structure.

In conclusion, GC-MS confirms the results from TLC that the green oily substrate has a complicated composition. More than 6 components present in the substrate. Mass spectra of these components are not conclusive to determine their structure, but suggest presence of diene isomers of $C_9H_{16}$. The possible assignments of some ion peaks are listed in Table 4.4.

**Table 4. 4. Possible assignments of the ion peaks identified by GC-MS (EI, +MS) in the organic phase product.**

| Ion peak | | Possible assignments | | | | |
|---|---|---|---|---|---|---|
| m/z | M+1 | Formula | mass | M+1 | Odd/even electrons | Possible Structures |
| 127.1 | 8.6 | $C_7H_{13}NO$ | 127.0998 | 8.3 | odd |  and other isomers |
| 124.1 | | $C_9H_{16}$ | 124.1253 | 10.1 | odd |  and other isomers |
| 109.1 | 8.3 | $C_8H_{13}^+$ | 109.1018 | 9.0 | even |  and other isomers |
| | | $C_7H_{11}N^{•+}$ | 109.0892 | 8.2 | even |  and isomers |
| 69.1 | 5.6 | $C_5H_9^+$ | 69.0705 | 5.6 | even |  and isomers |
| 59.0 | 2.8 | $C_2H_5NO^{•+}$ | 59.0372 | 2.68 | even |  |
| | | $C_2H_3O_2^+$ | 59.0133 | 2.32 | even |  |

In summary, the GC-MS analysis did not yield exact structures of the reaction product. However, it led to interesting fragmentations of the products which provided some implications on the reaction pathway. The ion at 127.1 (Figure 4.30, p181) has a formula of $C_7H_{13}NO$. One possible structure is a six-member-ring hydroxylamine shown in Table 4.4. The presence of compounds like this explains the EPR spectrum (Figure 4.17, p166) of the neutralized reaction mixture. At neutral pH, oxoammonium salt oxidizes hydroxylamines to the corresponding nitroxide radicals. The radical form of this compound has one α-hydrogen atom, which would give an EPR spectrum that matches the spectrum detected in neutralized reaction mixture. The ion at 124 can be assigned to $C_9H_{16}$ isomers, probably dienes, and possibly cyclic alkenes and alkynes. Their precise structure cannot be determined due to migration of double bonds. A peak at m/z=59.0 is present in many components. Taking into account the M/M+1 and rationality of the fragment, it is likely to be the radical cation of nitrosoethane, which has a formula of $C_2H_5NO^{•+}$. It is not likely to be $^+CH_2COOH$ because there is no peak at 45 ($[COOH]^+$), which is a distinctive ion fragment for carboxylic acid.

Similar ions were found in many components of the substrate. However, the molecular ions are all at low molecular weight. Electron impact is a hard ionization technique. It is possible that in some components, all peaks correspond to fragments. Therefore, a soft ionization technique (e.g. electrospray) is required to obtain more information about the molecular ions.

### 4.6.2.4.       MS: ESI

GC-MS by using EI ionization suggests some possible components in the green oily substrate. Although fragments of the components give some structural information, the molecular ions of the components have similar molecular weight. It indicates that the ionization technique is too harsh. Therefore, the substrate was analyzed by MS using electrospray ionization (ESI) technique. The mass spectrum is shown in Figure 4.35.
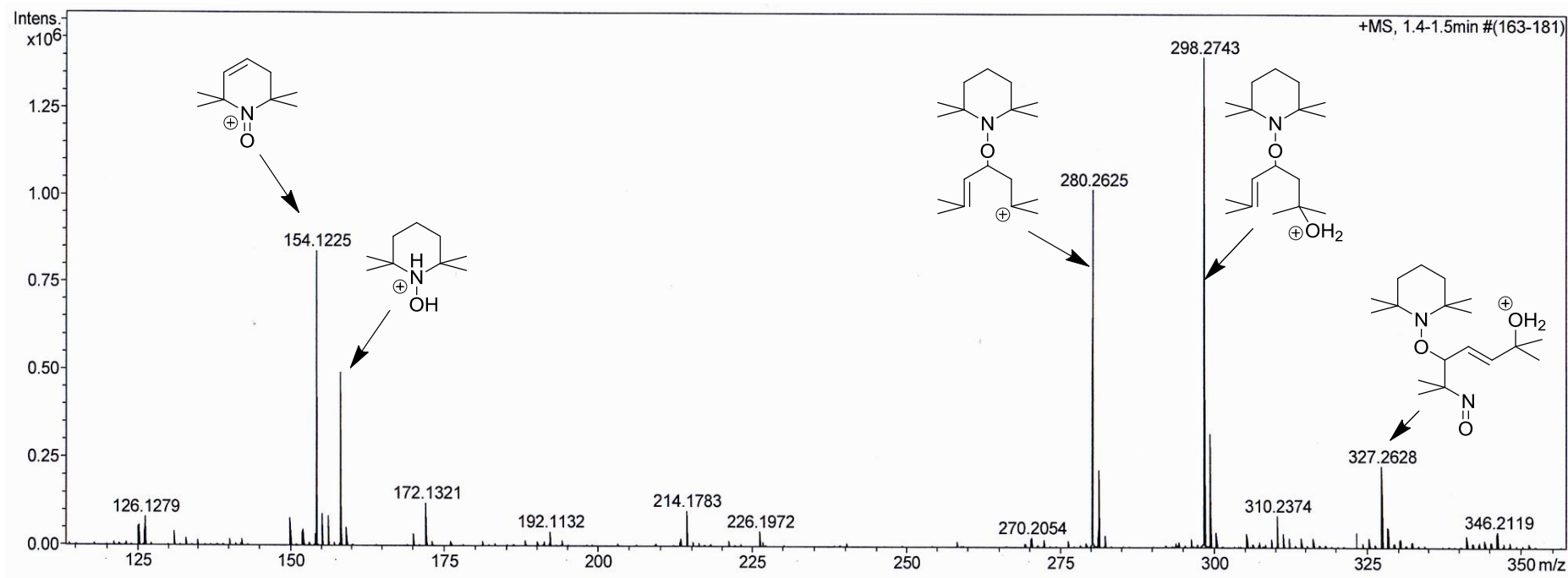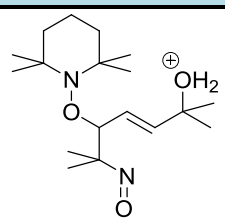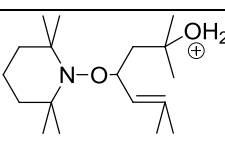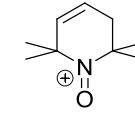
**Figure 4. 35. Mass spectrum (ESI, +MS) of the green organic substrate in trichloromethane.**

The green oily substrate contains several components. The substrate was analyzed without chromatography separation. Therefore the mass spectrum shown in Figure 4.35 is a mixture of different components. Major ions were thus analyzed and possible structures were obtained (Table 4.5)

**Table 4. 5. Possible assignments of the ion peaks identified by MS (ESI, +MS) in the organic phase product.**

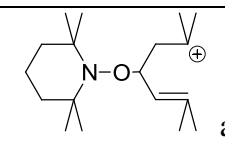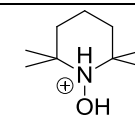| ion peak | | possible assignments | | | | |
|---|---|---|---|---|---|---|
| m/z | M+1 | formula | mass | M+1 | odd/even electrons | possible structures |
| 327.2628 | 23.4 | $C_{18}H_{35}N_2O_3$ | 327.2649 | 21.18 | even |  and isomers |
| 298.2743 | 22.8 | $C_{18}H_{36}NO_2$ | 298.2748 | 20.78 | even |  and isomers |
| 280.2625 | 20.9 | $C_{18}H_{34}NO$ | 280.2642 | 20.72 | even |  and isomers |
| 158.1537 | 10.1 | $C_9H_{20}NO$ | 158.1546 | 10.61 | even |  |
| 154.1225 | 11.1 | $C_9H_{16}NO$ | 154.1233 | 10.55 | even |  |

One of the distinctive peak in the mass spectrum is at m/z=158. It suggests the presence of TEMPO hydroxylamine which is consistent with the product analysis of the aqueous phase. TEMPO hydroxylamine is not a major component in the organic phase product. Major components are dimerization products. A small peak present at m/z=125 which corresponds to $C_9H_{16}$ dienes. The intensity is low because ionization of electron poor dienes is not efficient using electrospray. More importantly, the ion at m/z=154 indicates possible dimerization reaction pathways. TEMPO present in oxoammonium salt as an impurity. Hydrogen abstraction reaction to TEMPO explains formation of $C_9H_{16}NO^+$ (Scheme 4.15).
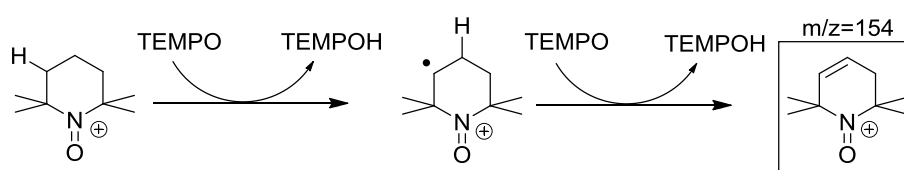


**Scheme 4. 15. Possible formation mechanism of $C_9H_{16}NO^+$ (m/z=154).**

Hydrogen abstraction from oxoammonium salt forms an alkyl radical on the piperidine ring, which can dimerize with another TEMPO molecule. Major components detected are ions at m/z=298 and m/z=280. A possible reaction mechanism is proposed in Scheme 4.16.
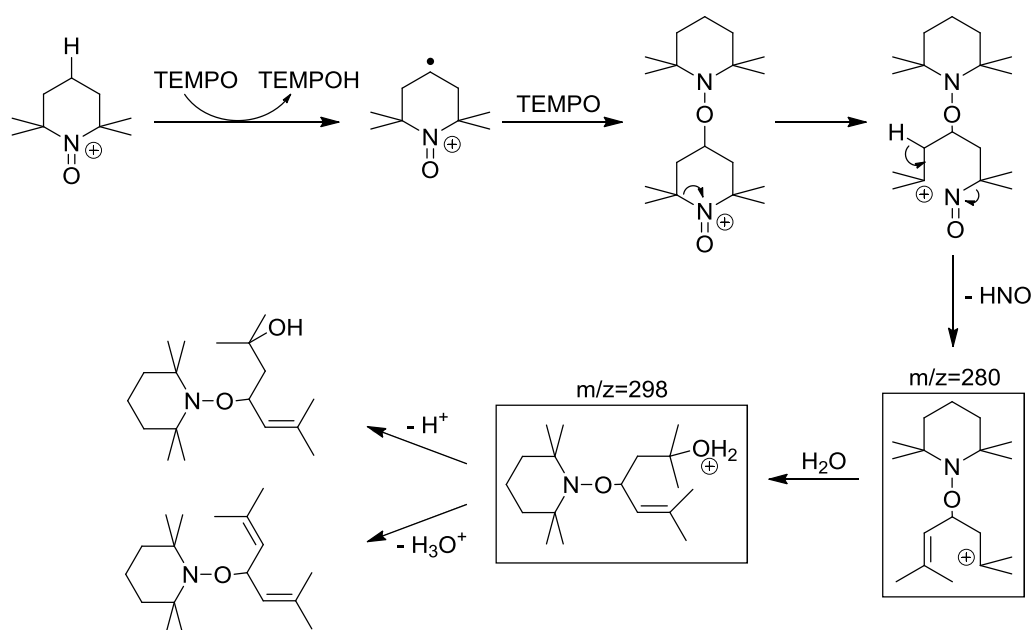


**Scheme 4. 16. Possible formation mechanism of $C_{18}H_{34}NO^+$ (m/z=280) and $C_{18}H_{36}NO_2^+$ (m/z=298).**

Alternatively, both TEMPO[13-15] and oxoammonium salt[16-17] can add to double bond and thus form a dimerization product. With similar ring opening mechanism, formation of ion at m/z=327 can be explained by Scheme 4.17.
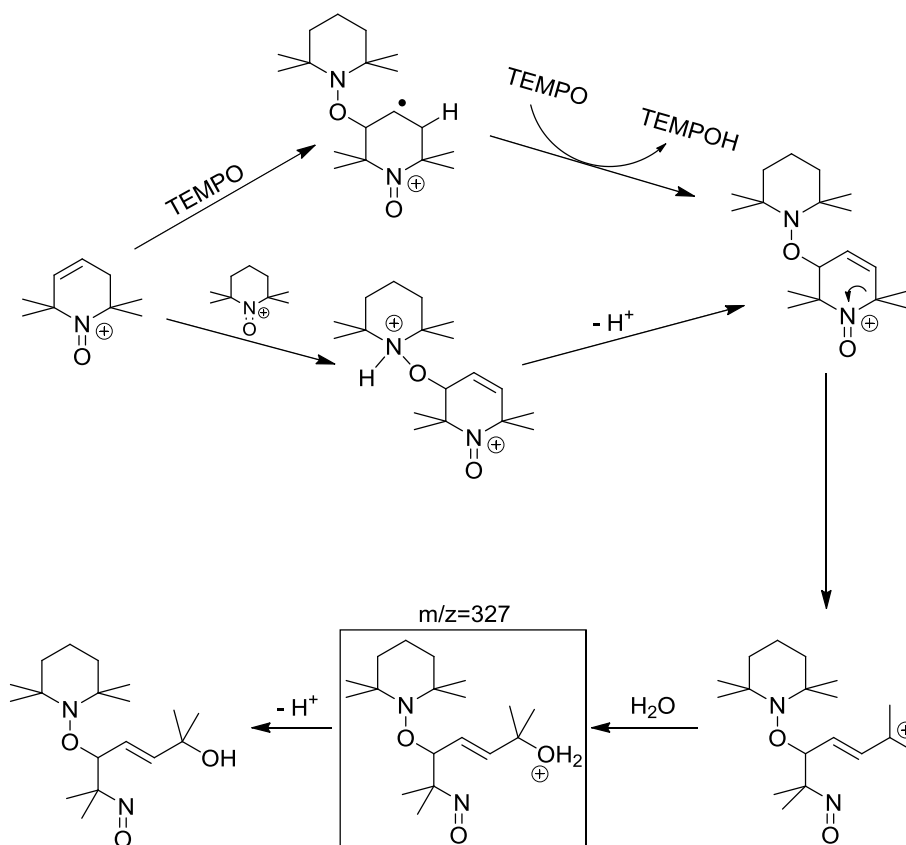


**Scheme 4. 17. Possible formation mechanism of $C_{18}H_{35}N_2O_3^+$ (m/z=327).**

This mechanism also includes formation of a C-nitroso compound. It explains the UV absorbance at *ca.* 670 nm and the green colour of the organic layer.

Therefore, investigation of the organic product by MS using electrospray ionization suggests a range of dimerization products are significant components in the mixture. The result also indicates that the mechanism of dimerization reaction includes formation of unsaturated bond on the piperidine ring followed by addition of TEMPO to the double bond.

**4.6.2.5.      NMR spectroscopy**

Mass spectrometry provides some valuable information about the structure of the products in the organic phase. Since the substrate is a mixture of several components, interpretation of its NMR spectra is complicated. However, NMR spectroscopy can be employed to confirm the presence of some functional groups. Therefore, the organic substrate was diluted in $CDCl_3$ and studied by $^1$H and $^{13}$C NMR spectroscopy. The spectra are shown in Figure 4.36.

a,                                    b,
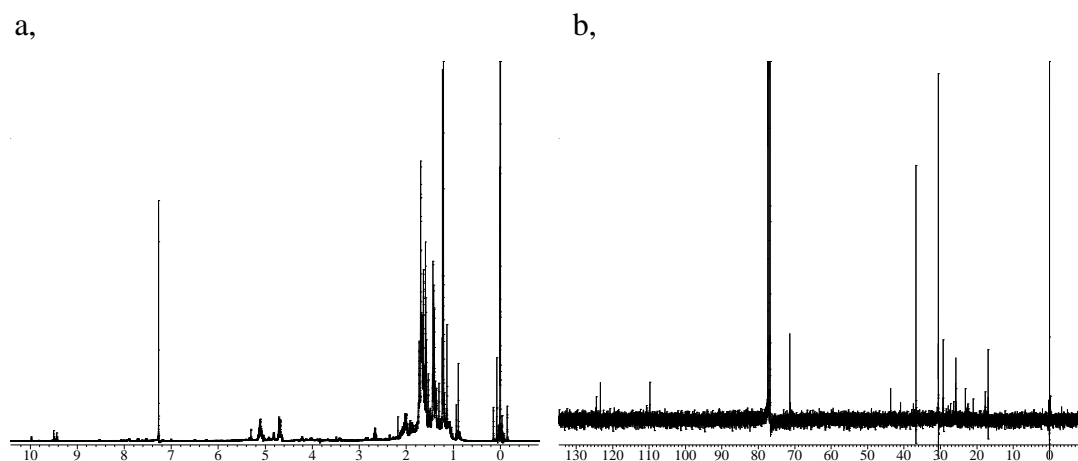


**Figure 4. 36. NMR spectra of the green organic substrate in CDCl$_3$. a, $^1$H. b, $^{13}$C.**

In $^1$H NMR spectrum, a multiplet at *ca.* 5 ppm was observed, which can be assigned to alkene protons. The singlet at *ca.* 1.7 ppm corresponds to the methyl groups adjacent to the double bond. The peaks at *ca.* 123 ppm in $^{13}$C NMR spectrum could be alkene carbons. This similarly confirms the presence of alkenes or dienes in the product. It is difficult to determine if the peak at *ca.* 110 ppm in $^{13}$C NMR spectrum is an alkene carbon or C1 of a nitrosoalkane. The signal at $\delta$=70 ppm corresponds to C1 of a hydroxylamine analogue (*e.g.* a dimerization product).

In conclusion, the composition of the organic substrate is complicated. It has more than 6 components according to GC and TLC studies. These components cannot be isolated due to small amount. Mass spectra of the organic substrate suggest dimerization products are important components in the mixture.

### 4.6.3.  Analysis of gas phase product

The gas phase product of the thermal decomposition of oxoammonium salt was also analyzed. As oxoammonium chloride decomposes, possible colourless gas phase products include CO, $CO_2$, $NO_x$ and volatile hydrocarbons. Therefore, to identify the product, GC and Infrared (IR) Spectroscopy was employed to carry out the head space analysis.

### 4.6.3.1. Analysis by GC-FID

In order to detect possible hydrocarbon products in the gas phase, head space analysis was carried out using gas chromatography (GC) with flame ionization detection (FID). This is a mature method to detect volatile hydrocarbons from methane to C12 compounds. $1.05 \times 10^{-3}$ mol oxoammonium chloride was dissolved in 0.8mL $H_2O$ and transferred to a pipette which was sealed using a rubber septum. The sample was degassed using a frozen-thaw method and filled with $N_2$. Then the oxoammonium chloride solution was heated at 100 °C for 25 min. Gas sample was collected from the head space of the cooled reaction mixture using a 250 μL gas syringe. The gas sample was injected to the GC-FID system for analysis. No signal was detected. The detection limit of the analyzing system for 1 litre sample is between 2-9 ppt (v/v), therefore for 250 μL sample the detection limit is *ca.* 1ppm. Hence, the result suggests absence of hydrocarbons in the gas phase product.

### 4.6.3.2. Analysis by gas phase IR

Since hydrocarbons were not detected in the head space, it leaves CO, $CO_2$ and $NO_x$ as possible products. Since many of these molecules have distinctive infrared (IR) spectra, gas phase IR was used to analyze the head space. A similar preparation method was used to collect the gas on the headspace and transfer to a gas phase IR cell. Approximately 3mL gas was obtained from heating of $1.05 \times 10^{-3}$ mol oxoammonium salt at 80 °C for 20 min. The IR spectrum was thus obtained (Figure 4.37).

*Identification of $CO_2$ in the gas phase product*

The IR spectrum of the gas phase product displays a doublet at *ca.* 2350cm$^{-1}$ which overlaps with the $CO_2$ signal in the background. This signal originates from $CO_2$ in the product but not background, as can be seen from the ratio of the $CO_2/H_2O$ peaks in the products (Figure 4.37a) and a blank cell (Figure 4.37b).
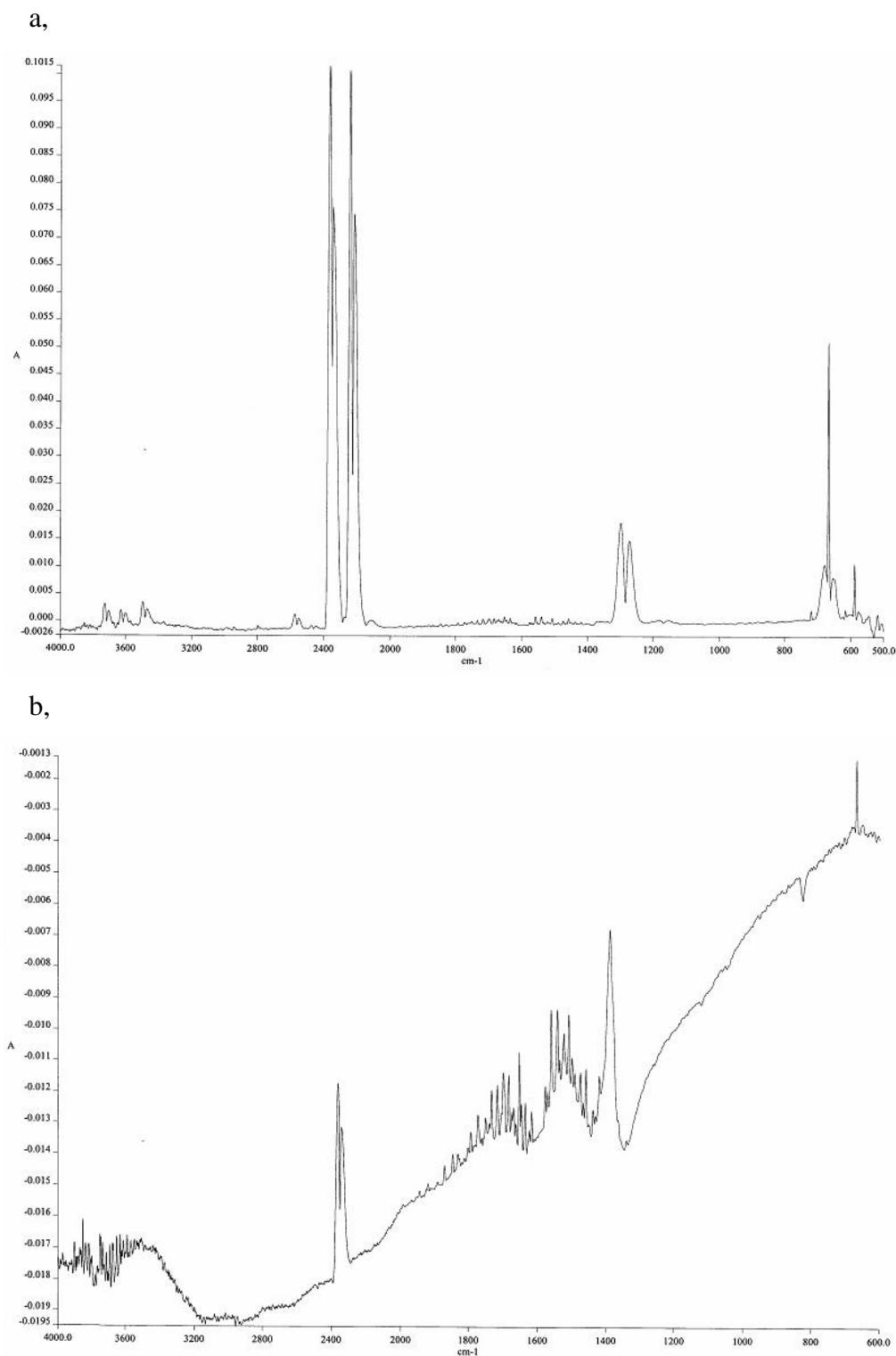
a,

b,

**Figure 4. 37. IR spectra of the gas phase product (a) and air background (b) in absorbance.**

*Identification of N₂O in the gas phase product*

Apart from the $CO_2$ signal, the other intense peaks include the doublets at 2212/2236 cm$^{-1}$ and 1272/1299 cm$^{-1}$ (Figure 4.38, red spectrum). These peaks are consistent with the distinctive IR spectrum of nitrous oxide ($N_2O$).[18] The two absorbance bands correspond to the asymmetric and symmetric stretching of $N_2O$.

Therefore, to confirm the spectral assignment, an authentic sample of $N_2O$ gas was generated via thermal reaction of $NH_4NO_3$. $CO_2$ was also prepared via reaction of sodium hydrogen carbonate with sulphuric acid. The $N_2O$ and $CO_2$ gases were mixed in a 1:1 (v/v) ratio and injected into a gas-tight IR cuvette cell. The IR spectrum of $N_2O + CO_2$ mixture is very similar to the IR spectrum of the head space product. In fact, the two spectra overlap very well (Figure 4.38) which suggests $N_2O$ and $CO_2$ are the components of the gas phase product.



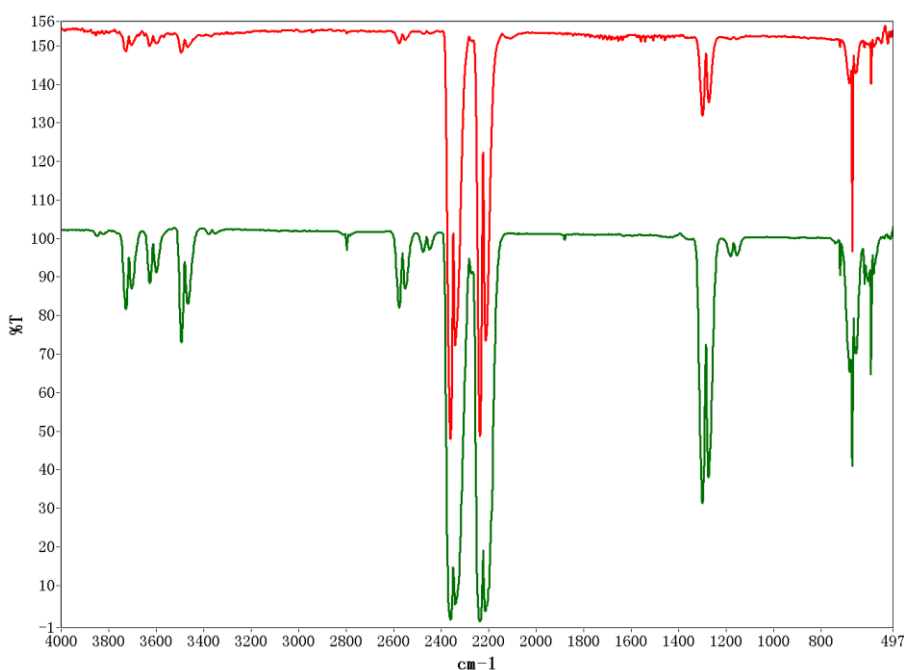**Figure 4. 38. Overlaid IR spectra of head space product of thermal decomposition of oxoammonium chloride (×5, red) and 1: 1 (v/v) CO₂ + N₂O gas (green).**

*Determination of the ratio of N₂O and CO₂ in the gas phase product*

In the IR spectrum of a 1:1 (v/v) $CO_2$ + $N_2O$ mixture, the peaks at *ca.* 2350 cm$^{-1}$ and 2230 cm$^{-1}$, which correspond to $CO_2$ and $N_2O$, respectively, have similar intensity. The intensity of these peaks can thus be used to estimate the ratio of these two components. In the IR spectrum of head space product, these two peaks also have similar intensity. Therefore, the molar ratio of $CO_2$ and $N_2O$ can be estimated to be 1:1 in the gas phase product.

At room temperature, the water solubility of $CO_2$ and $N_2O$ is 1.45 g/L and 2.2 mg/L, respectively. As a result, in 0.8 mL solution, dissolved $CO_2$ and $N_2O$ are $2.64 \times 10^{-5}$ mol and $4 \times 10^{-8}$ mol, respectively.

Therefore, the yield of $CO_2$ and $N_2O$ can be calculated from the IR intensity and water solubility of the gases. $1.05 \times 10^{-3}$ mol oxoammonium salt yielded $9.34 \times 10^{-5}$ mol $CO_2$ (gas 1.5mL, $6.70 \times 10^{-5}$ mol, dissolved $2.64 \times 10^{-5}$ mol) and $6.70 \times 10^{-5}$ mol $N_2O$ (gas 1.5mL, $6.70 \times 10^{-5}$ mol, dissolved negligible).

## 4.7.    Conclusions

In the product analysis of thermal decomposition of oxoammonium chloride, nearly 10 reaction products were identified. The products are distributed in the aqueous, organic and gas phase. In the aqueous phase, formation of hydroxylamine is determined using NMR spectroscopy and by titration of the aqueous reaction mixture. TEMPO hydroxylamine is the major components in the aqueous phase product. A small amount of nitrate was detected using Ion Chromatography.

The gas phase products have been identified as $CO_2$ and $N_2O$ using gas phase IR spectroscopy. The molar ratio of these two components is approximately 1:1. Volatile hydrocarbons were not detected in the gas phase product.

The organic phase product was formed in small amount, but it has a complex composition, with more than 6 components present in the product. Many different dimerization products were detected. In many cases, precise structures of the product were not determined but the general structural features were identified. The reaction

products provided much information on the possible reaction pathways and mechanism.

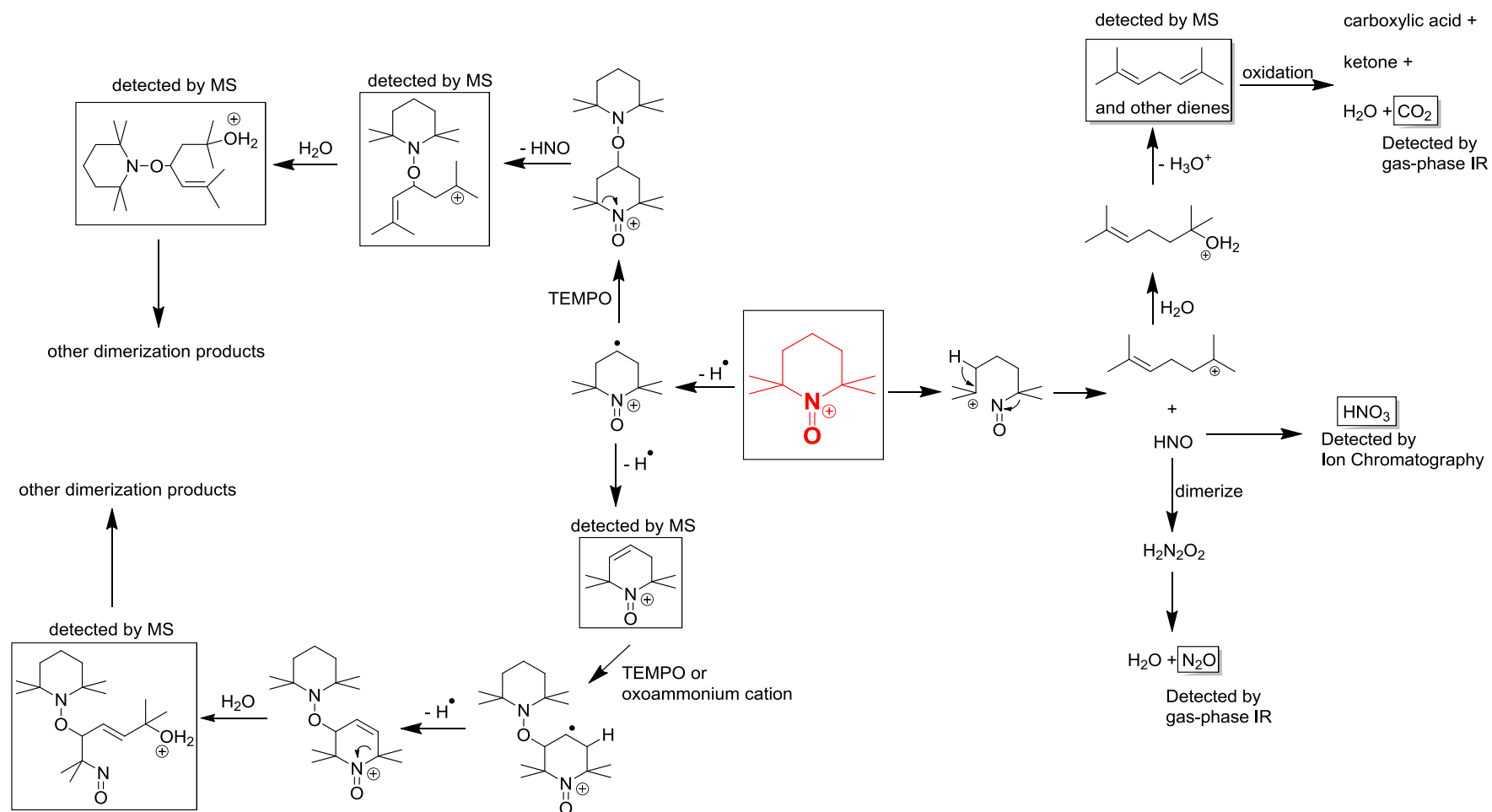### 4.7.1. Mechanism of thermal decomposition of oxoammonium salt

The major reaction products of thermal decomposition of oxoammonium chloride are TEMPO hydroxylamine, $CO_2$, $N_2O$ and dimerization products such as $C_{18}H_{33}NO$. The formation of hydroxylamine from oxoammonium salt is a reduction reaction. This reaction can be due to oxidation of unsaturated hydrocarbons to $CO_2$ in the presence of oxoammonium salt. Formation of $N_2O$ explains the presence of unsaturated hydrocarbons in the product. Elimination of nitroxyl (HNO) from oxoammonium salt produces alkenes. HNO is reactive towards nucleophiles and quickly dimerizes to hyponitrous acid, $H_2N_2O_2$, which is then dehydrated to nitrous oxide $N_2O$ (Scheme 4.18).[19-20] The rate of the dimerization reaction was reported to be $8 \times 10^6$ $M \cdot s^{-1}$.[21] HNO and the conjugated base $NO^-$ form an acid/base pair with $NO^-$ being isoelectronic with dioxygen. The biochemistry[22-24] of the $HNO/NO^-$ pair has drawn much attention due to the potential medical applications.

$$HNO \xrightarrow{\text{dimerize}} H_2N_2O_2 \longrightarrow H_2O + N_2O$$
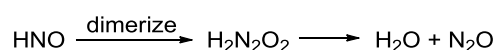
**Scheme 4. 18. Formation of $N_2O$ from HNO.**

Formation of HNO probably also explains the presence of $NO_3^-$ in the aqueous phase, as an oxidation reaction of HNO can be presumed.

Therefore, a mechanism of the thermal decomposition of N-oxoammonium salt is proposed (Scheme 4.19).

**Scheme 4. 19. Proposed mechanism of decomposition of N-oxoammonium salt.**

In the proposed reaction mechanism, ring-opening of oxoammonium salt leads to elimination of HNO and a carbocation. HNO dimerizes to form hyponitrous acid $H_2N_2O_2$, which then dehydrates to form $N_2O$ and $H_2O$. The carbocation formed can be hydrolysed and further eliminates to yield isomers of 2,6-dimethylhepta-1,5-diene. The dienes can be oxidized to forms carboxylic acid, ketone, $CO_2$ and water.

Dimerization products can be formed via addition to alkyl radical or to unsaturated bond on the piperidine ring, following hydrogen abstraction reaction from oxoammonium salt.

## 4.7.2. Yield calculations and mass balance

Thermal decomposition of oxoammonium salt is evidently a complex reaction, which involves nearly 10 reaction products. The yields of the main products are discussed in this section. All yields are presented in molar percentage. TEMPO hydroxylamine is the major product. Its yield is *ca.* 60%, determined by titration of aqueous phase product and NMR spectroscopy. About 4% $NO_3^-$ was also detected in the aqueous phase. In the gas phase, yield of $N_2O$ is 6.4%, which corresponds to *ca.* 13% of the oxoammonium salt. The organic layer contains several components which may include dimerization products and isomers of $C_9H_{16}$ diene. Since isolation of each component is not possible, it's difficult to calculate the exact yield. By an estimation, the organic layer accounts for less than 4% weight ratio of the starting material. If a single component, $C_{18}H_{33}NO$, is assumed to be the only product in the organic phase, the yield would be 7.2%. In reality, the yield is probably lower. The products in aqueous, organic and gas phase add up to a total yield of *ca.* 85%. Purity of the staring material, oxoammonium salt, is *ca.* 95% according to CHN analysis. Considering the fact that products in different phases were studied separately that may enlarge experimental error, this total yield is reasonable.

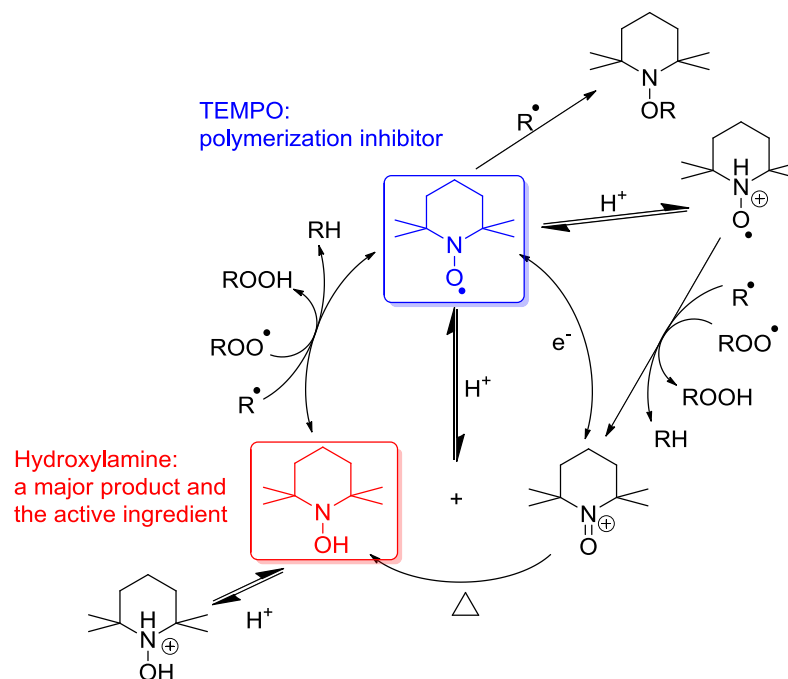### 4.7.3. Mechanism of TEMPO decay in acid at high temperature

Thermal decomposition of oxoammonium salt was investigated and a reaction mechanism is proposed. The mechanism provides a missing piece of TEMPO decay in acid at high temperature (e.g. 100 ℃). The full mechanism of acid-catalyzed TEMPO decay at high temperature is proposed in Scheme 4.20. TEMPO is protonated in acid, and followed by a disproportionation reaction to yield the corresponding hydroxylamine and oxoammonium salt. Ring opening of N-oxoammonium cation leads to formation of HNO and dienes, which eventually forms $N_2O$ and $CO_2$ gas. In this process, oxoammonium salt is the oxidizing agent and is reduced to form hydroxylamine. In the overall reaction mechanism of TEMPO decay, the yield of hydroxylamine can be over 75% hence it is the major product of this reaction.
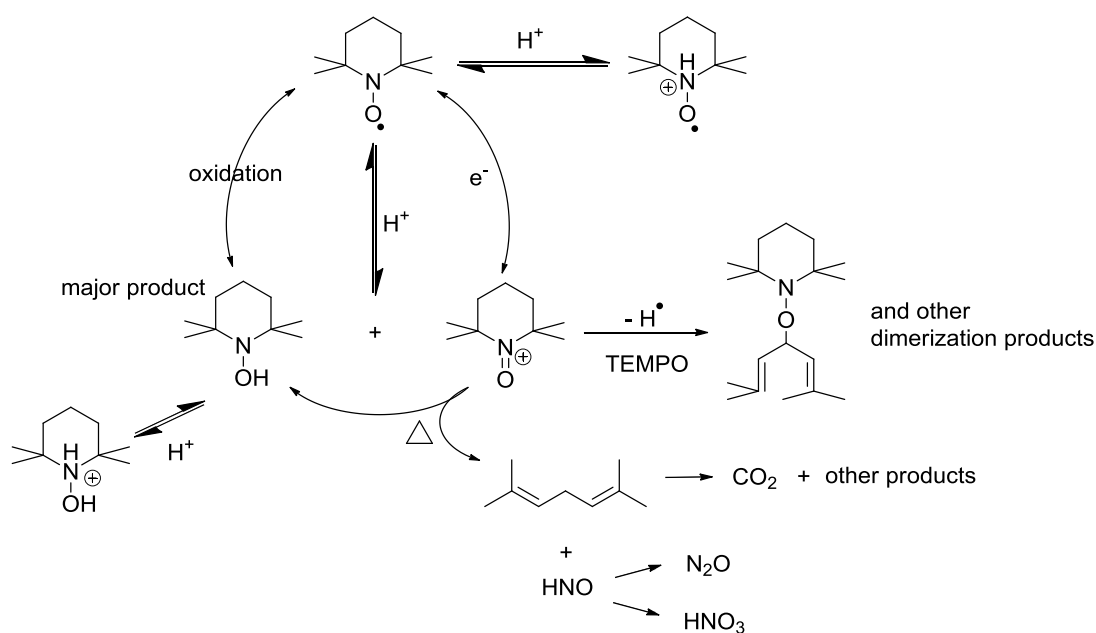


**Scheme 4. 20. Mechanism of TEMPO decay in acid high temperature**

In the spontaneous polymerization system of acrylic acid, TEMPO can undergo the same reactions which lead to accumulation of hydroxylamine as a major product. Hydroxylamine itself can act as an antioxidant via reactions with alkyl and peroxyl radicals, and forms TEMPO in the process. Therefore, a low concentration of TEMPO is maintained in the spontaneous polymerization system of acrylic acid. This may be responsible for the inhibition efficiency of TEMPO in acids. The

antipolymerant effect of TEMPO is achieved via its reaction with alkyl radicals, or via the reaction of peroxyl and alkyl radicals with protonated TEMPO. The inhibition mechanism of TEMPO in acrylic acid is described in Scheme 4.21.



**Scheme 4. 21. Antioxidant reactions of TEMPO in acid at high temperature.**

### 4.7.4. Perspectives and future work

Since hydroxylamines are in fact the active ingredient in the inhibition mechanism, it is possible to use different types of hydroxylamines in a mixture with phenols to develop novel polymerization inhibitors. In addition, the decomposition of oxoammonium salt provides a relatively clean conversion from TEMPO or oxoammonium salt to TEMPOH. This reaction may be useful in antioxidation systems. Formation of nitroxyl (HNO) and $N_2O$ from oxoammonium salt can be utilized for potential medical applications. Future work may include utilize the understandings of the reaction mechanisms investigated, possibly in developing novel polymerization inhibitor mixtures and $N_2O$-releasing oxoammonium salts (*e.g.* catalyzed decomposition).

**References:**

1. M. V. Ciriano, H. G. Korth and W. B. V. Scheppingen, *J. Am. Chem. Soc.*, 1999, **121**, 6375-6381.

2. V. A. Golubev, É. G. Rozantsev and M. B. Neiman, *Russ. Chem. Bull.*, 1965, **14**, 1898-1904.

3. V. A. Golubev, G. N. Voronina and E. G. Rozantsev, *Russ. Chem. Bull.*, 1970, **19**, 2449-2451.

4. J. F. W. Keana and F. Baitis, *Tetrahedron Lett.*, 1968, 365-&.

5. Y. L. Chow, J. N. S. Tam and K. S. Pillay, *Can. J. Chem.*, 1973, **51**, 2477-2485.

6. G. Grampp and K. Rasmussen, *PCCP*, 2002, **4**, 5546-5549.

7. T. D. Lee and J. F. W. Keana, *J. Org. Chem.*, 1975, **40**, 3145-3147.

8. V. D. Sen, V. A. Golubev and N. N. Efremova, *B. Acad. Sci. USSR Ch.*, 1982, **31**, 53-63.

9. W. H. Koppenol and J. F. Liebman, *J. Phys. Chem.*, 1984, **88**, 99-101.

10. J. L. Hodgson, M. Namazian, S. E. Bottle and M. L. Coote, *J. Phys. Chem. A*, 2007, **111**, 13595-13605.

11. C. Lagercrantz, *Free Radical Res. Com.*, 1991, **14**, 395-407.

12. K. Murayama and T. Yoshioka, *Bull. Chem. Soc. Jpn.*, 1969, **42**, 2307-2309.

13. F. Aldabbagh, W. K. Busfield, I. D. Jenkins and S. H. Thang, *Tetrahedron Lett.*, 2000, **41**, 3673-3676.

14. J. E. Babiarz, G. T. Cunkle, A. D. DeBellis, D. Eveland, S. D. Pastor and S. P. Shum, *J. Org. Chem.*, 2002, **67**, 6831-6834.

15. A. D. Allen, B. Cheng, M. H. Fenwick, W.-w. Huang, S. Missiha, D. Tahmassebi and T. T. Tidwell, *Org. Lett.*, 1999, **1**, 693-696.

16. P. P. Pradhan, J. M. Bobbitt and W. F. Bailey, *Org. Lett.*, 2006, **8**, 5485-5487.

17. K. M. Church, L. M. Holloway, R. C. Matley and R. J. Brower, *Nucleos. Nucleot. Nucl.*, 2004, **23**, 1723-1738.

18. T. M. Miller and V. H. Grassian, *J. Am. Chem. Soc.*, 1995, **117**, 10969-10975.

19. M. N. Hughes and H. G. Nicklin, *J. Chem. Soc. A*, 1971, 164-168.

20. P. S. Y. Wong, J. Hyun, J. M. Fukuto, F. N. Shirota, E. G. DeMaster, D. W. Shoeman and H. T. Nagasawa, *Biochemistry*, 1998, **37**, 18129-18129.

21. V. Shafirovich and S. V. Lymar, *Proc. Natl. Acad. Sci. U.S.A.*, 2002, **99**, 7340-7345.

22. K. M. Miranda, *Coord. Chem. Rev.*, 2005, **249**, 433-455.

23. J. C. Irvine, R. H. Ritchie, J. L. Favaloro, K. L. Andrews, R. E. Widdop and B. K. Kemp-Harper, *Trends Pharmacol. Sci.*, 2008, **29**, 601-608.

24. N. Paolocci, M. I. Jackson, B. E. Lopez, K. Miranda, C. G. Tocchetti, D. A. Wink, A. J. Hobbs and J. M. Fukuto, *Pharmacol. Ther.*, 2007, **113**, 442-458.